BRNO UNIVERSITY OF TECHNOLOGY
VYSOKÉ UČENÍ TECHNICKÉ V BRNĚ

FACULTY OF CHEMISTRY
FAKULTA CHEMICKÁ

INSTITUTE OF PHYSICAL AND APPLIED CHEMISTRY
ÚSTAV FYZIKÁLNÍ A SPOTŘEBNÍ CHEMIE

NOVEL MATERIALS FOR ORGANIC AND HYBRID ELECTRONICS AND PHOTONICS
NOVÉ MATERIÁLY PRO ORGANICKOU A HYBRIDNÍ ELEKTRONIKU A FOTONIKU

SUMMARY OF DOCTORAL THESIS
AUTOREFERÁT DIZERTAČNÍ PRÁCE

AUTHOR Ing. Matouš Kratochvíl
AUTOR PRÁCE

SUPERVISOR prof. Ing. Martin Weiter, Ph.D.
ŠKOLITEL

BRNO 2022

ABSTRAKT

Obor organické elektroniky nabízí jedinečnou možnost masové výroby levné a ekologicky přívětivé elektroniky. Otevírá dveře novým funkcím a tvarům zařízení, které standardní elektronika na bázi kovu a křemíku neumožňuje.
Možnosti dané povahou organických látek a pokrok ve výzkumu syntézy nás zásobují novými materiály pro fotonické aplikace. Hlavní motivací této práce je hledání nových materiálů a zkoumání vztahu mezi jejich molekulární (a krystalickou) strukturou a vlastnostmi.
Tato práce je zaměřena na studium optických a/nebo elektrických vlastností nových materiálů pro fotonické aplikace. Materiály prezentované v práci jsou organické i hybridní organicko-anorganické, u nichž je snaha získat to nejlepší z obou světů. Výzkum prezentovaný v této práci se skládá ze tří samostatných částí, které jsou propojeny cílem studovat vztah mezi strukturou materiálu a jeho vlastnostmi a metodami používanými ke studiu těchto vlastností.
První část si klade za cíl představit materiály vykazující účinnou fluorescenci v pevné fázi (Solid-State Fluorescence, SSF). V této práci jsou prezentovány dvě série materiálů vykazujících SSF. Barva emise je řízena změnami skupin přitahujících elektrony v push-pull systémech molekul. Výsledky ukazují efektivní (>10%) emise pokrývající většinu viditelného spektra (~450–650 nm).
Druhá část prezentovaného výzkumu zkoumá vliv thionace na známou skupinu nízkomolekulárních polovodičů – diketopyrrolopyrrolů (DPP). Prezentované výsledky ukazují ve studovaných molekulách výraznou preferenci n-typové chování následkem thionace, s řádovým zvýšením pohyblivosti elektronů, a také působivě nízko ležící hladiny LUMO (~ −4,5 eV).
Třetí část uvedených výsledků je zaměřena na perovskitové materiály pro fotonické aplikace. Hybridní materiál – organo-olovnato-halogenidový perovskit je již téměř půldruhého desetiletí v centru pozornosti výzkumníků v oblasti pokročilé fotoniky. Perovskitové solární články prokazují pozoruhodnou účinnost, avšak jejich využití stále brání problémy se stabilitou. V této práci je prezentována studie stability jako referenční bod pro další výzkum v této oblasti a pro získání vhledu do procesů ovlivňujících stabilitu perovskitových materiálů a solárních článků. Následně je navržen a otestován přístup ke zvýšení stability a výkonu článků, využívající materiály studované ve druhé studii.

ABSTRACT

The field of organic electronics offers the unique possibility of mass production of cheap and environmentally friendly electronics. It opens doors to novel functionalities and device forms not possible with the standard metal- and silicon-based electronics.

The possibilities given by the nature of organic compounds and progress in synthetic research supply new materials for photonic applications. The search for novel materials and the investigation of the relationship between the molecular (and crystalline) structure and properties of the material are the main motivation of this thesis.

This thesis is focused on study of optical and/or electrical properties of novel materials for photonic applications. The materials presented in the thesis are both organic and hybrid organic-inorganic ones, trying to get the best of both worlds. The research presented in this thesis comprises three distinct parts interconnected by the aim to study the relationship between the structure of material and its properties and by the methods used to study these properties.

The first part aims to present efficient solid-state fluorescent (SSF) materials. In this thesis two series of SSF materials are presented. The colour of the emission is controlled by varying the electron withdrawing groups in the push-pull systems of molecules. The results show efficient emission (>10 %) covering most of the visible spectrum (~450–650 nm).

The second part of the research investigates the effect of thionation on the well-known small-molecule group of semiconductors, diketopyrrolopyrroles (DPPs). The presented result shows a notable preference for n-type behaviour upon thionation with increase of electron mobilities by orders of magnitude, as well as impressively low lying LUMO levels (~ −4,5 eV) in the studied molecules.

The third part of the presented results aims at perovskite materials for photonic applications. The hybrid material, organo-lead-halide perovskite, has been the center of attention of researchers interested in advanced photonics for almost a decade and half. The perovskite solar cells have shown remarkable efficiency, however, their utilization is still hindered by stability issues. A stability study is presented as a reference point for further research on this topic and to gather insight into processes influencing the stability of perovskite material and solar cells. Then an approach to increase the stability and performance of the cell is proposed and tested utilizing materials studied in the second study.

KLÍČOVÁ SLOVA

π-konjugované materiály, organická elektronika, optické vlastnosti, elektrické vlastnosti, fluorescence v pevné fázi, diketopyrrolopyrroly, organické polovodiče, perovskit, perovskitová fotovoltaika

KEYWORDS

π-conjugated materials, organic electronics, optical properties, electrical properties, solid-state fluorescence, diketopyrrolopyrrols, organic semiconductors, perovskite, perovskite photovoltaics

TABLE OF CONTENTS

1 INTRODUCTION

The worldwide importance of organic electronics is constantly growing, with OLED technologies utilized by corporations such as Samsung, Sony, Apple, etc., and also OPV technologies are successfully entering the market industrialized by companies such as Heliatek, Oxford PV or Organic Electronic Technologies (OET). Despite having its roots in the 1970s, organic electronics is still a fast growing and dynamic field of research, and recently also industry. As such, there is a high demand for novel materials that can push the limits and improve performance. This thesis is dedicated to the search for such materials.

Organic electronics is a broad term that encompasses various technologies. Some are now well established and are being utilized, such as organic light-emitting diodes (OLEDs) and organic photovoltaics (OPV). Some are well-known but their potential has not yet been fully exploited, e.g. organic field-effect transistors (OFETs) which offer ambipolar charge transport unlocking new possibilities in multifunctional digital circuits. Some are lately fast emerging, such as organic electrochemical transistors (OECTs), which show great potential in the field of bioelctronics. The materials are frequently utilized also in optical applications, for example as colorants, luminescent probes, two-photon polymerization initiators, etc.

Organic materials offer a unique pairing of semiconducting and optical properties together with easy ways to tweak them (via means of synthesis). Other advantages over inorganic semiconductors lay in better compatibility with living tissues and organisms (for bioelectronics) and the possibility of processing them from solution by printing techniques (low cost, low energy, low losses). From the customer-centred point of view, the possibility to produce flexible, patterned, and to great extent colour-tuned products is non-negligible and in some instances (wearable electronics) almost necessary.

However, organic electronics have not yet reached the long-term efficiency and lifetime associated with inorganic materials, although this is balanced by easier waste management and recycling at the end of life. Life cycle analysis shows low energy payback times, making organic electronics a “green” technology. Considering everything said above, it is reasonable to assume that organic electronics will soon surpass traditional inorganic electronics in specialized and more targeted applications.

In the modern world, where more and more attention is given to green energy, environmentally friendly products, waste and energy savings, but also to easy applicability and comfort of use, organic electronics offer great opportunities.

This thesis focuses on the study of the relationship between the structure and properties of novel organic compounds and their potential utilization in optical and optoelectronic applications. The aim is not to synthesise new materials but to characterize them, assess, and verify their possible applications, and provide knowledge, which may be then utilized in designing new materials. In the first part

of the thesis, the theoretical background and current knowledge in the field is researched and briefly summarized. The following chapter presents the experimental approach to the scientific work itself, outlining the studied properties and methods used. The final part summarises the results of experiments carried out with the perspective of assessing the properties of novel materials as well as their utilization in optoelectronic devices.

The research is divided into three studies; the first one deals with two series of solid-state emissive materials, the second is targeted at a group of organic semiconducting pigments, and the last is focused on perovskite photovoltaics and its possible improvements by use of organic semiconductors. The key element connecting these studies is the characterization of materials and the investigation of the underlying structure-properties relations.

2 CURRENT RESEARCH RELATED TO THE THESIS

2.1 Solid-state fluorescent materials

As is often observed, materials that are highly emissive in solution show only weak or even no emission in the solid state. The aggregation-caused quenching (ACQ) is considered disadvantageous in many applications (fluorescent markers, OLED emitters, two-photon printing initiators, etc.). On the other hand, in some applications, i.e. where high charge carrier mobility is crucial, ACQ is usually the first sign of beneficial interactions in the solid state. However, the focus of relevant chapters in this thesis (**5.1** and **5.2**) is the search for efficient solid-state emitters. The ways to achieve solid state emission (SSF) are non-covalent – targeting beneficial packing in the aggregate state [1]; or covalent – by modification of the molecule (attaching bulky substituents or chemical modification of the core itself) to prevent aggregation of molecules [2]. To prevent π–π stacking interaction among neighbouring molecules, leading to efficient SSF, one of two approaches is used. The first utilizes a partially or fully twisted core structure [3], the second relies on introduction of steric hindrance by bulky substituents close to the core [4].

In the field of solid-state emissive materials, there is still one great challenge – efficient far-red/near-infrared (FR/NIR) emission. Solid-state organic luminophors emitting in this spectral region (FR/NIR, 650–900 nm) find their application especially in the fields of OLED and bioimaging [5]. For an emitter to show red emission, a narrow HOMO-LUMO gap is required. This is usually achieved by polycyclic aromatic molecules with an extended π-system or by π-conjugated molecules substituted by electron-donating and electron-withdrawing groups. However, materials with such low HOMO-LUMO gap tend to have lower solid-state fluorescence quantum yields than materials emitting at shorter wavelengths. To look closer at the donor-acceptor design of FR/NIR emitters, the linking is usually done in D-π-A, D-π-A-π-D or A-π-D-π-A fashion. The donor (D) in these structures is usually a di- or triphenylamino group (DPA, TPA), and the acceptors (A) are a heterocyclic accepting moiety, two or more cyano (CN) groups or a combination of both. A quantification of required properties of FR/NIR emitters was given by Shimizu and Hiyama in 2010 expressed the need to obtain materials with red emission showing PLQY over 30% from neat solids [6]. It was they themselves who, in 2012, for the first time, presented material with emission with a maximum of emission over 700 nm (702 nm) and PLQY over 30% (33%) simultaneously [7].

In this thesis, the stilbene-based structure will be studied in D-π-A system with DPA donor and various acceptors, with the aim of constructing solid-state emitters based on one fluorophore that cover a large part of the visible spectrum and producing accessible material that breaks the >700 nm; >30 % limit.

2.2 Semiconducting materials

The performance of devices is always limited by the properties of the materials used. With almost limitless possibilities given by the diversity of organic materials, there is an ongoing search for new functional materials. The materials are evaluated on the basis of the properties required for the intended application, e.g. high absorptivity, mobility of charge carriers, fluorescence wavelength and quantum yield, etc. An important factor is also how well the materials will work in combination; some of the properties that have an effect are energy levels' positions, structural features affecting arrangement in solid state, or solubility in various solvents. An important place among the building blocks of organic semiconductors is held by diketopyrrolopyrrole (DPP)-based molecules.

2.2.1 Structure of di(thio)ketopyrrolopyrrole

Diketopyrroloprrole (2,5-dihydropyrrolo[3,4-*c*]pyrrole-1,4-dione) is a molecule first reported by Farnum [10] and subsequently commercialized as industrial pigments by the Ciba-Geigy company in the 1970s. It forms the core of DPP derivatives most commonly being substituted by aromatic moieties such as phenyl or thiophenyl (Ph-DPP and Th-DPP). These aryls are part of the conjugated system and thus affect optical and electrical properties. However, the torsion angles between the DPP core and the aryl moieties influence the electronic coupling. If nitrogen atoms in 2,5 positions are left unsubstituted (2,5-dihydro form), the material is in the pigment form (highly insoluble).

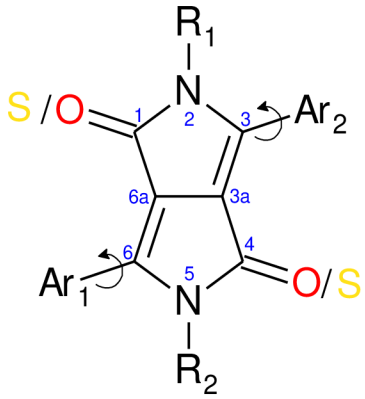

Figure 1 The structure of diketopyrrolopyrrole with atom numeration. $Ar_{1,2}$ denotes the possible substitution of aryl in positions 3 and 6, $R_{1,2}$ denotes the possible substitution of alkyl in positions 2 and 5. The torsion angles (α, β) between aryls and DPP core are highlighted. Possible thionation is indicated.

It was discovered that N-alkylation leads to solubilisation of DPP derivatives, because the intermolecular H-bonding ensures strong interactions in the solid state. The resulting DPP dyes showed strong fluorescence [11]. Although alkyls do not contribute to the π-system, they do have an impact on it. Repulsive interactions have been observed between N-alkyls and aryls in 3,6 positions, which leads to rotation of aryls outside of the molecular plane and hypsochromic shift [12]. N-alkylation

also has a great impact on packing in solid state [13]. It is important to mention that differences of packing translate to the properties of resulting solid state material. Good example is influence of introducing adamantane group as a $R_{1,2}$ substituent in Ph-DPP described by Kovalenko *et al.* [14].

2.2.2 Properties and applications of di(thio)ketopyrrolopyrroles

The relatively simple synthesis, combined with interesting properties and easy ways of modification, led to great attention and extensive investigation of DPP derivatives. The majority of the research aims to use DPP materials as organic semiconductors, e.g. in organic field effect transistors (OFETs), organic solar cells (OSCs) or organic light-emitting diodes (OLEDs) [15–17]. However, due to their outstanding emission and stability, DPP materials are also studied as fluorescent probes, lasing media in dye lasers or two photon absorbing dyes [18–20]. A large portion of DPP-related research is aimed at the utilization of the DPP unit as a part of polymer materials. Here, however, most focus will be given to small-molecule applications. The research of the use of DPPs in OFETs has undergone fast development. In 2008, Yanagisawa *et al.* reported a hole mobility of $1{,}43 \cdot 10^{-5}$ $cm^2V^{-1}s^{-1}$ in Ph-DPP pigment [21]. And after just 6 years, electron and hole mobilities as high as $1 \cdot 10^{-2}$ $cm^2V^{-1}s^{-1}$ were observed in highly ordered thin films of Ph-DPP [22]. In OSCs with DPP-based donors, the best conversion efficiencies are usually achieved using DPP-based polymer materials, reaching over 10 % [23], but also cells utilizing small molecule donor DPPs reached efficiency over 5 % [24, 25]. In the search for a suitable replacement of expensive fullerenes, which are usually used as acceptors in record-breaking devices, also DPP-based materials were studied. Some of the highest efficiencies (even over 15 % in ternary cells) using small molecule DPP acceptor were reported by Privado *et al.* [26].

A possible, although not widely studied, way to modify the DPP motif is to substitute the ketone oxygen with sulphur, thus forming thioketone. The resulting compound is referred to as dithioketopyrrolopyrrole (DTPP). It was first synthesized in the mid 1980s as part of ongoing research of DPPs by researchers at Ciba-Geigy [27]; the synthesis was also reported as independently discovered by F. Closs and R. Gompper [28]. Synthesis is a simple single-step reaction using a thionation agent (e.g. Lawson's reagent). The synthesized and subsequently studied DTPP molecule was 1,4-dithioketo-3,6-diphenyl-pyrrolo-[3,4-*c*]-pyrrole (**Ph-DTPP**) pigment. In a series of papers at the turn of 80s and 90s J. Mizuguchi and his colleagues have shown some interesting properties of this particular molecule [29]. As was easily observable upon synthesis and then confirmed by recording of the absorption spectrum, thionation had lowered the band gap in comparison with the parent molecule (Ph-DPP), and the parent red pigment was transformed into a dark blue one. Then, J. Mizuguchi *et al*. focused on changes in packing of DTPP thin films upon vapour treatment, which brought about an increase in absorption and photoconduction in near-infrared. They comprehensively studied this phenomenon and came up with several possible applications such as the use in laser printers and

memory devices [29–31]. Since publication of this intensive study, not a great deal of attention, in comparison with DPPs, has been paid to DTPP based molecules. Nevertheless, some highly intriguing works have been published investigating the influence of sulphur substitution on the molecule. Unique visible and near-infrared halochromic and halofluoric properties were discovered in *S*-alkylated DTPP-based molecules and polymers. This feature is attributed to the more basic nature of the present nitrogen compared to the lactam one in DPP, which enables acid-base reaction [32]. Solutions of DTPP-based dyes (*S*-alkylated) and polymers also show reversible thermochromism in visible and near-infrared at temperatures ranging from room temperature to 120 °C [33]. All the reported results are in agreement with the fact that thionation reduces the band gap. From cyclic voltammetry measurements it has been shown that it is due to especially stabilizations of LUMO level and also by destabilization of HOMO. This effect occurs in both DTPP dyes and polymers [34–37]. The same influence was observed in isoDPP/isoDTPP (isoDPP is a regioisomer of DPP, in which the positions of carbonyl and amide are exchanged). Moreover, authors report a shift from p-type to ambipolar behaviour of isoDTPP based polymers in OFETs [38]. On the other hand DTPP based polymers have shown promising results as hole-transporting materials for perovskite solar cells, bringing increased stability in comparison to the widely used spiro-OMeTAD [37]. No reports on the mobility in small molecule DTPP could be found. Additionally, to the best of our knowledge, no new results concerning DTPP pigments were published since the work of Mizuguchi *et al*.

The above-mentioned state-of-the-art motivated us to study the optical and semiconducting properties of two representative DTPP pigments (Th-DTPP and Ph-DTPP). More precisely, we were interested in whether these compounds are capable of forming stable, low band gap, low LUMO n-type semiconductors with potential to be used in organic optoelectronics.

2.3 Perovskite materials for photonic applications

The stoichiometry of perovskite compounds is ABX_3, where A and B are cations of different sizes and X is an anion (**Figure 2**). Perovskite materials can be classified by their chemical composition, with different anions and cations. Out of these various classes, the most interesting from the point of view of energy photogeneration is the class of hybrid organo-lead halide perovskites. These consist of halide anion (I^-, Br^-, Cl^-), lead cation (Pb^{2+}) and small organic cation (mostly methylamonium – MA and/or formamidinium – FA).

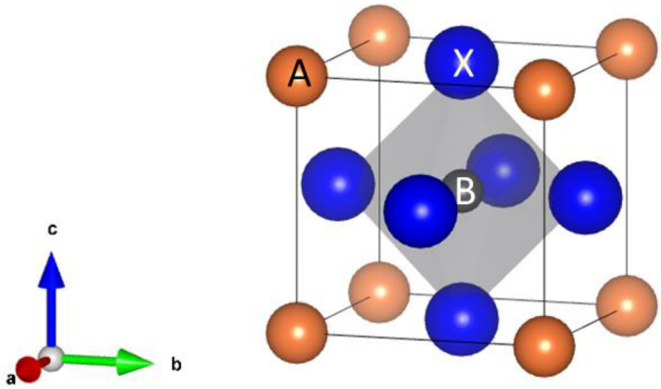

Figure 2 Unit cell of perovskite structure. Produced using Vesta software [39].

In 2009, organometallic halide perovskites were reported as sensitizers in the visible light region for dye-sensitized solar cells. Miyasaka *et al.* were the first to fabricate a perovskite solar cell based on the mesoporous TiO_2 photoanode sensitized by $MAPbX_3$ (X = I, Br). The photovoltaic cells had only modest PCE values $\eta = 3{,}8$ % (iodide) and 3,1 % (bromide) but have shown high voltage ($U_{OC} \approx 0{,}9$ V). However, the cells were stable only for a few minutes [40]. A major turning point in perovskite photovoltaic research came in 2012, when a ground-breaking all-solid-state perovskite sensitized solar cell was prepared with the organic solid-state hole transport layer formed by spiro-MeOTAD. This device achieved a PCE of 9,7 % and significantly increased stability (from a few minutes to around 500 hours) [41]. This publication started intensive research and during 2013 several papers were published that describe the increase in efficiency of PSCs, mainly due to the optimisation of preparation. By the end of 2013, the published record efficiency exceeded 15% [42]. Planar architecture cells were also developed achieving efficiencies comparable to those of dye sensitised cells [43]. The absorber material used in the vast majority of these studies was $MAPbI_3$. This unusually fast development has sparked widespread interest in the field of perovskite photovoltaics as well as perovskite materials in general. As a result, record efficiency had steadily increased.

2.3.1 Photogeneration of charge in OSC and PSC

The process of photogeneration in heterojunction OSC is illustrated in **Figure 3**. In OSCs, the light is absorbed by an active layer formed by donor and acceptor materials. As described earlier, upon absorption, an electron is promoted from HOMO to LUMO; in organic materials the electron and hole pair remains tightly bound in the form of exciton. The binding energy of the exciton is relatively high (0,3–1 eV) [44]. For OSC to function and produce photocurrent, the exciton must be separated into free charge carriers. Charge separation takes place at the donor-acceptor (D-A) interface – heterojunction. The migration of exciton to the D-A interface is a diffusive process with exciton diffusion length in organic materials is in the range of 1–20 nm [45], in polymers usually around 10 nm [46]. If the exciton

does not reach the D-A interface, it decays back to the ground state. After the dissociation the free charge carriers are transported towards electrodes where they are extracted [45].

The process of charge photogeneration is different in PSC as is illustrated in **Figure 3**. On the contrary to OSCs, the absorption in the perovskite active layer in PSCs does not lead to the formation of a strongly bound exciton. In various studies, the exciton binding energy in perovskite material has been reported to be in the range of few meV. Such low binding energies mean that absorption practically generates free charge carriers [47–49]. The non-excitonic nature of charge photogeneration is one of the keys to PCS's high performance. The much more efficient free charge carrier generation in comparison to OSCs is a crucial advantage, as significant energy losses are connected with exciton migration and separation. The charge separation in PSC occurs by injection of photogenerated electrons into ETL and holes into HTL. This means that the charge carrier generated near the opposite charge transport layer has to diffuse through the whole active layer, which increases the chance of recombination. However, a large photoinduced dielectric constant has been reported for $MAPbI_{3-x}Cl_x$ perovskite material [50]. The high dielectric constant removes coulomb attraction between carriers and facilitates ambipolar transport by effective charge screening [51].

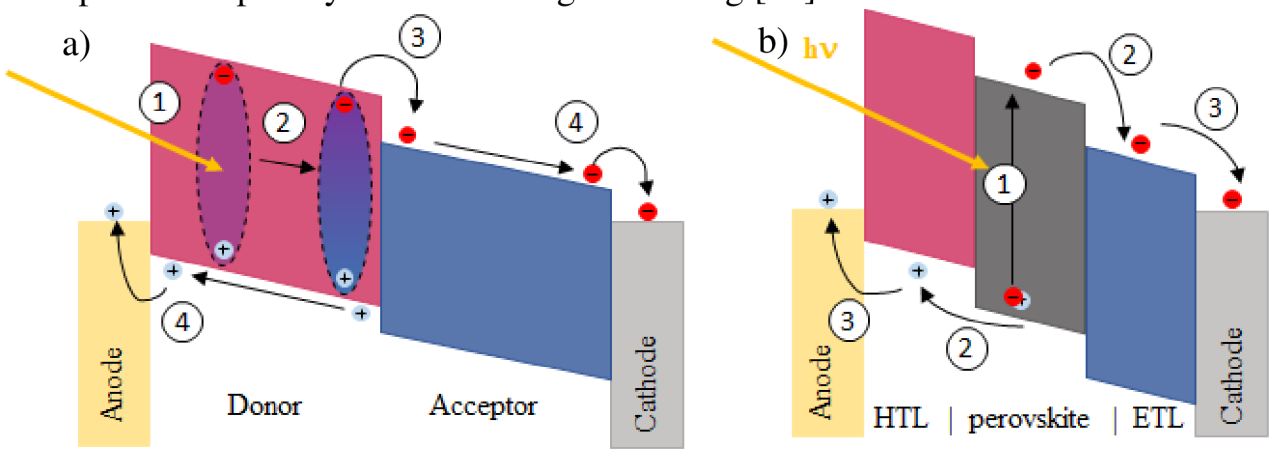

Figure 3 (a) Scheme of function of an organic solar cell. (1) absorption of photon and exciton generation; (2) exciton diffusion to the donor-acceptor interphase; (3) charge separation and transfer between donor and acceptor, generation of free charge carriers; (4) transport of charge carriers to electrodes and their extraction. (b) Scheme of function of a perovskite solar cell. (1) absorption of photon and generation of free charges; (2) transport of charge carriers to the electrode interface; (3) charge extraction.

The role of research in the field of π-conjugated materials for applications in organic and perovskite solar cells has not diminished even nowadays. Research of the utilization and optimization of large-scale production techniques, such as printing and large area coating, has made it possible to produce solar cells in large quantities. This naturally increased the pressure to find alternatives for high-cost materials. There is also a search for materials with better stability or improvements

in the stability of contemporary devices. Organic photovoltaics was overshadowed by perovskite solar cells for a decade. However, in recent years we have witnessed a renaissance of the field of organic solar cells. It is related to the achievements in search for efficient NFAs for the bulk heterojunction. Due to novel accepting materials, higher PCEs were achieved [52–54].

Novel organic semiconductors are studied as part of this thesis. The materials exhibit an n-type behaviour and a potential to be used as NFAs in organic solar cells or as transport and passivation layers in perovskite solar cells.

2.3.2 Perovskite material issues addressed in this work

Solar cells and other photonic devices based on perovskite materials show remarkable efficiencies which are still growing; on the other hand, the stability is still an issue hindering their full utilization. The first major step in improving stability was the utilization of the above mentioned all-solid-state cells. Since then new insight in the processes crucial for the stability has been acquired. Moisture has been identified as a key element in degradation, being able to completely disturb the perovskite structure [55]. Another issue that is in the spotlight of perovskite-related research is the problem of interfaces. Optimization of multiple interfaces present in devices has become a primary tool for harnessing the full potential of perovskite-based optoelectronics [56]. For example, the addition of a layer of organic material to the PSC stack has been shown to lead to an almost 10% increase in power conversion efficiency [57].

The perovskite-related research described in this thesis aims to address the stability. A degradation study will be used to study the relationship between the structure and morphology of materials and their properties and ability to withstand external influences causing degradation. A huge effect is also expected from optimization of PSC manufacturing, such as deposition conditions, post-deposition treatment, or use of auxiliary materials. Possible synergy with other parts of the research is actively sought for. Both optically active and semiconducting materials may have a beneficial effect. The utilization of organic semiconductors in PSC may bring improvements in both the stated issues – stability and interface optimization.

3 AIMS OF THE THESIS

The general aim of the conducted work described in this thesis was to study the relationship between the molecular structure of advanced organic and hybrid compounds and their optical, electrical, and optoelectrical properties. The studied properties are closely related to the intended applications such as use as solid-state fluorescent materials and active or auxiliary materials in organic electronic devices, i.e. organic field-effect transistors or solar cells. The technological aspect of the final devices, i.e. the device structure and fabrication, is also an issue addressed in this

work. This approach brings about the set of tasks paving the way to achieve the set goals:

- Study the optical properties of the material in solution.
- Study optical properties in the solid state, inspect how the properties of isolated molecules (solution) translate into the properties of aggregated systems.
- Discuss the possible applications of materials based on recorded properties.
- Study the optoelectronic properties and morphology of materials selected for applications in devices.
- Prepare prototypes of devices and study their parameter and/or influence of the environment on them.
- Prepare devices with the introduction of new materials and study the influence on stability.

The π-conjugated materials used in photonic applications share some same and some similar structural features, whether the intended application is purely optical or optoelectronic. As a result, the same methods are used and mostly the same properties are studied. Although, depending on the intended application, some of the expressed properties might be viewed as either beneficial or detrimental.

Optical characterization is a powerful tool in studying the structure-properties relationship of novel materials. For optoelectronic materials, the shape and position of absorption as well as its strength (quantified as molar absorption coefficient) are crucial. For most applications, strong absorption is vital, as more absorbed photons translate to more molecules in excited states. The absorption maximum wavelength then determines which part of the spectrum may be used to excite this material, or which part will be filtered upon passing through it. The fluorescence of the material is equally important. Ranging from the colour of the light emitted to the efficiency of the fluorescence. The interaction between the same molecules in aggregated state or between different molecules can also be studied by the means of optical methods. The interactions (or lack thereof) are expressed as quenching of fluorescence. The fluorescence lifetimes of materials were studied by time-resolved fluorescence spectroscopy, which can provide insight into the processes that take place in the material. The optical properties of the materials were studied in solutions and in the solid state.

The bandgap (or HOMO-LUMO gap) of the material is an important parameter, which can be estimated from the absorption spectrum. However, the right alignment of the energy levels of neighbouring materials in the optoelectronic device is crucial for its performance. Thus, the values of energy of the HOMO and LUMO bands (orbitals) are required. To obtain these, different techniques than absorption spectroscopy are needed. In this work, the electrochemical approach was used. In this way, the oxidation and reduction potentials are determined and the HOMO and LUMO potentials are calculated.

For optoelectronic application of the studied material, charge carrier mobilities are an important parameter with a decisive influence on the resistance of the layers

in devices. The type of major charge carrier also determines the use of material in the devices. For example, p-type materials are used as hole transporting layers and donors in active layer of heterojunction solar cells, whereas n-type materials are used as electron transporting layers and acceptors (in heterojunction solar cells). Electrical characterization was conducted to obtain insight into the behaviour of the material in relation to electric current. The charge carrier mobilities were studied in field-effect transistor devices.

The detailed characterization of pure material, both optical and electrical, in solution and solid state gives necessary information on the structure-properties relationship. This insight is crucial for the future design of novel derivatives and tailoring of their properties.

In organic and hybrid optoelectronic devices, there is an underlying challenge of device stability over longer time periods and especially in various environmental conditions. To properly address this issue, the stability study was conducted in a controlled environment. Such a study provides the necessary information on the rate of degradation processes and allows the study of technological approaches aimed at slowing degradation. The influence of environment may be studied by electrical characterization of the device performance as well as by more detailed characterization of particular parts of the device by crystallographic and optical methods.

To fulfil the goals of determining the properties of novel materials outlined above, experimental methods and approaches described in the next chapter were used.

Optimization of some of the methods and implementation (or development) of others is an integral part of the research. This is due to the utilization of novel materials and scientific progress, placing new demands and opening new possibilities in the field of material research. The outcome of this work, along with the new discoveries, is also building a knowledge base regarding the structure-properties relations and broadening of the institutional know-how in our research team.

4 METHODOLOGY

In this work novel materials were studied for applications in organic electronics and photonics. Such research includes thorough characterization of synthesized materials (with advantageous feed-back loop to the synthesis team) first in solutions, then solid state and final testing in devices. Each step of the characterization gathers information that is used in the next one. It must be noted that not all investigation have been carried out by the author. Density functional theory (DFT) calculations used to predict properties and gain insight into the underlying processes were performed by Dr. Luňák, single-crystal X-ray diffractometry (XRD) measurements of the SSF materials were performed by Prof. Růžička's team at UPCE, single-crystal XRD measurements of DTPPs were carried out by Dr. Fábry's group at the Institute of Physics of the Czech Academy of Sciences, and XRD characterization of perovskites by Dr. Chladil at FME, BUT. The help of all colleagues is gratefully appreciated.

Characterization of novel materials may sometimes pose a challenge to standard methods of characterization. Consequently, some methods had to be optimized for used samples, and new methods had to be implemented. For example, a laboratory setup for measurement of two-photon absorption has been designed and put into practice.

4.1 Optical properties

Optical properties were studied in solutions (as separated molecules) of various solvents and in the solid state (thin films or polycrystalline powder samples). Absorption and fluorescence spectroscopy were used to gather information about the energy structure of excited and ground states of materials (absorption and emission bands), as well as about their interactions with the surrounding environment (solvent molecules or other molecules of the same material) and resulting solvatochromism (-fluorism), and interactions in solid state. The time-correlated single photon counting (TCSPC) technique was used to record PL decay using of SSF materials (chapters **5.1** and **5.2**).

4.2 Electrical and electrochemical properties

Current-voltage (I-V) characteristics measurements were used to test the performance of finalized lab-scale devices (solar cells) in the research of perovskite materials for photonic applications (chapter **5.4**). The measurements were carried out in dark and under illumination. The basic parameters of the solar cells were derived from I-V characteristics. These were namely short-circuit current density (j_{sc}), open-circuit voltage (V_{oc}) and maximum power output (P_{max}), values of fill factor (FF) and power conversion efficiency (PCE, η) were calculated according to

equations (1) and (2). Typical I-V characteristics of solar cell is depicted in **Figure 4**.

$$\eta = \frac{P_{max}}{P_0} = \frac{|U_{max}\ I_{max}|}{P_0} = \frac{|U_{oc}\ I_{sc}|\ FF}{P_0}, \tag{1}$$

$$FF = \frac{P_{max}}{U_{oc}\ I_{sc}} = \frac{|U_{max}\ I_{max}|}{|U_{oc}\ I_{sc}|}. \tag{2}$$

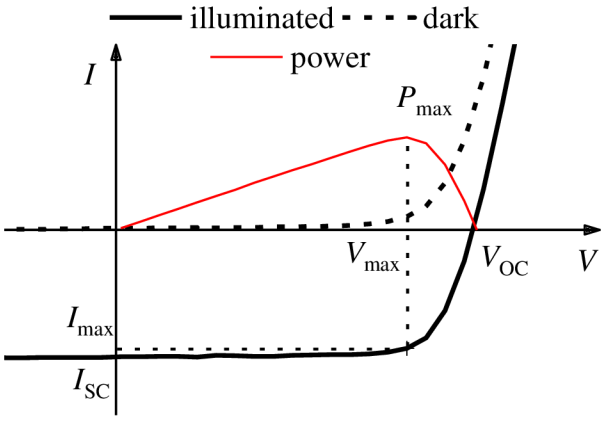

Figure 4 An example of typical current-voltage characteristic of a solar cell under illumination (black line) and in the dark (dashed line) and the corresponding power output (red line). Positions of important points are marked on the axes (short-circuit current – I_{SC}, open-circuit voltage V_{SC}, the current and voltage giving maximal power P_{max} – I_{max} and V_{max}).

The depiction of connection and parameters of OFET device are depicted in **Figure 5**.

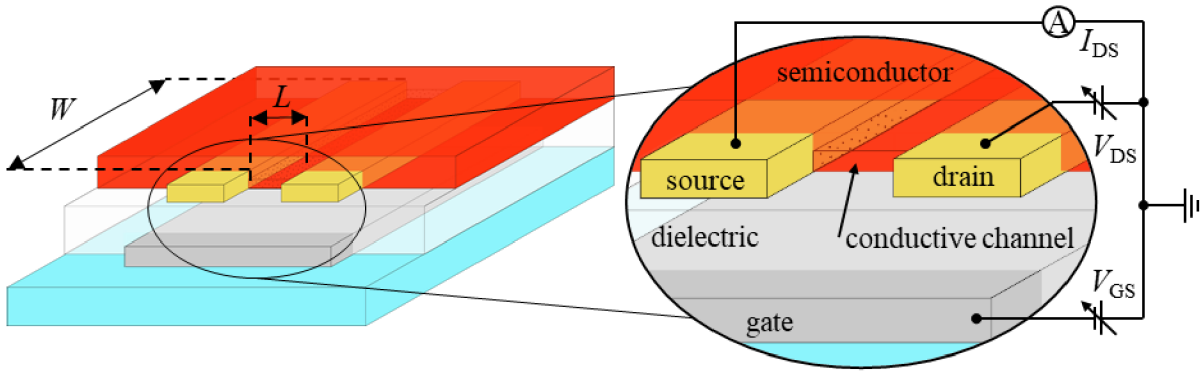

Figure 5 Depiction of the geometric parameters of the transistor channel, W is the width and L the length (left) and schematic representation of the electrical connection and basic parameters of the OFET device, I_{DS} is the electric current flowing through the organic semiconductor, V_{DS} is the voltage applied between the source and drain electrodes and V_{GS} is the voltage applied between the gate and source electrodes.

The field-effect charge carrier mobilities of studied D(T)PP compounds (chapter **5.3**) were determined by characterization of organic field-effect transistors (OFETs). The OFETs were operated in accumulation mode and charge carrier mobilities were calculated from the saturation region of transfer characteristics according to the equation (3).

$$\mu = 2\frac{L}{W \cdot C_{\mathrm{d}}}\left(\frac{\sqrt{I_{\mathrm{DS}}}}{\mathrm{V_{GS}} - V_{\mathrm{th}}}\right)^2 . \qquad (3)$$

To estimate the positions of the HOMO and LUMO levels of studied D(T)PP compounds (chapter **5.3**), electrochemical measurements of thin films were carried out. The external standard – ferrocene/ferrocenium redox couple was used to calibrate the setup. This couple has a reduction potential of 0,69 V vs. normal hydrogen electrode (NHE) in acetonitrile solution [58]. The calculated correction value was +411 mV from potential vs. Ag/AgCl QRE to potential vs. NHE. Energy levels were calculated using the following formulas from onset potentials [59]:

$$E_{\mathrm{HOMO}} = -(4{,}75\ \mathrm{eV} + E_{\mathrm{ox,onset}}\ \mathrm{vs\ Ag/AgCl} + 411\ \mathrm{mV}), \qquad (4)$$

$$E_{\mathrm{LUMO}} = -(4{,}75\ \mathrm{eV} + E_{\mathrm{red,onset}}\ \mathrm{vs\ Ag/AgCl} + 411\ \mathrm{mV}), \qquad (5)$$

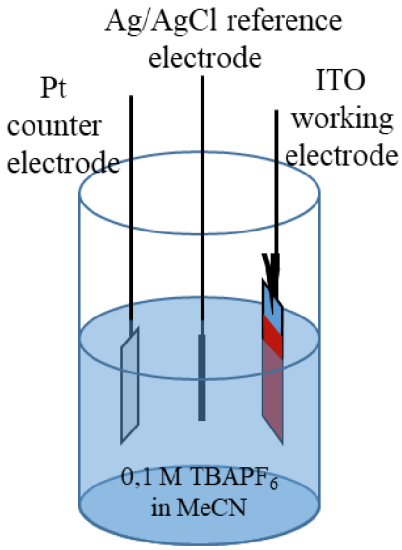

Figure 6 The experimental setup for cyclic voltammetry measurement of thin film samples.

4.3 Sample preparation

The preparation of samples for optical measurements (solutions, powder samples, thin films) was conducted in the chemical laboratory under ambient conditions (room temperature ~25 °C, atmospheric pressure, humidity in the range of 20–40 % RH).

The thin films for optical characterization were deposited on cut glass slides either by spin coating or by physical vapour deposition (PVD) in the PVD Handy (Vaksis) evaporator.

The samples for cyclic voltammetry were evaporated onto ITO coated glass substrates using the PVD Handy.

Various procedures were implemented to try to influence the solid-state packing of studied materials either in the form of a powder sample or a thin film. These include temperature and solvent annealing, and application of pressure (powder samples only).

The substrates for thin films and for devices were always cleaned by the same procedure. This consists of subsequent sonication in different baths for 10 to 15 minutes and rinsing. The routine is as follows: bath of NaOH solution or basic detergent, rinsing with deionized water, deionized water bath, rinsing with dry air/nitrogen, acetone bath, rinsing with isopropyl alcohol (IPA), IPA bath, and drying with dry air/nitrogen.

To investigate the morphology of thin films of the studied materials, mechanical profilometry and atomic force microscopy (AFM) were used. These method were utilized in the parts of research in which thin films were studied, i.e. study of D(T)PPs and perovskite materials (chapters **5.3** and **5.4**). The AFM was used to investigate the topography of thin films. The thickness of the fabricated thin films was measured mechanical profilometer (Bruker).

4.3.1 Device fabrication

For preparation of solar cells, a class C clean room was utilized to minimize the presence of dust and other impurities that decrease the performance of the final devices. The clean room is equipped with MB-200B MBRAUN glove boxes (M. Braun Inertgas-Systeme) filled with nitrogen (O_2 and H_2O content <1 ppm) and a dry air box in which controlled humidity is achievable. The oxygen-sensitive materials were handled exclusively in the nitrogen gloveboxes.

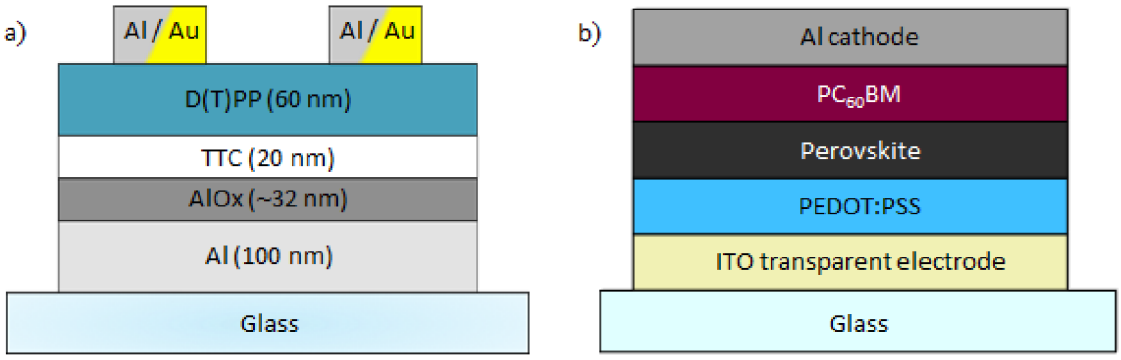

Figure 7 Device architecture of (a) organic field-effect transistor (OFET) and (b) perovskite solar cell (PSC).

The prepared functional devices were of two types. OFETs (chapter **5.3**) and PSCs (chapter **5.4**), their structures are depicted in **Figure 7**. OFETs in this work were used as a tool to investigate material property – field-effect mobility of charge

carriers (holes and electrons), PSCs are used to test photovoltaic properties of perovskite material and how they are influenced by various factors (moisture, addition of passivation layer, etc.).

The device preparation consists of many steps and each one of them has significant influence on the whole device performance. This means that device optimization is a long and challenging process. The optimization of preparation of PSCs was also part of this work, although the process is not described here and the results presented come from optimized devices.

4.4 Studied materials

4.4.1 Diphenylamino-diphenylstilbenes

The novel molecules synthesised by partners at Faculty of Chemical Technology, University of Pardubice consist of a stilbene core substituted by an electron donating group diphenylamine (DPA) and different electron withdrawing groups (EWGs), creating a push-pull system of D-π-A type. The π-system is substituted by two phenyls at the acceptor part, resulting in 2,5-diphenyl-stilbene (DPS). The acceptor (EWG) groups are vinyl (V), dibromovinylene (DBrV), cyano (CN), aldehyde (CHO), and dicyanovinylene (DCV).

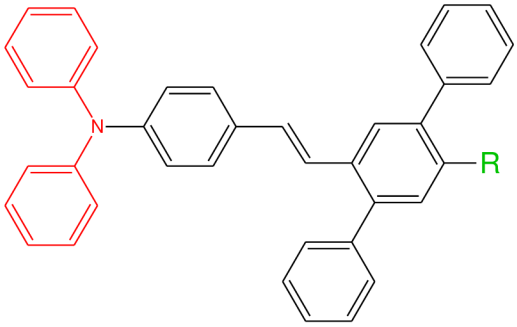

designation	DPA-DPS-V	DPA-DPS-DBrV	DPA-DPS-CN	DPA-DPS-CHO	DPA-DPS-DCV
R =	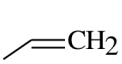	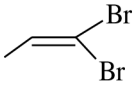	—CN	—CHO	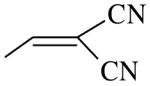

Figure 8 The studied diphenylstilbenes push-pull systems end-capped on one side by diphenylamine (electron donor, red) and on the other by various electron withdrawing groups (green).

4.4.2 Diphenylamino-diphenyl-distyrylbenzenes

The novel molecules synthesised by partners at Faculty of Chemical Technology, University of Pardubice are a continuation of the series of molecules presented in the previous chapter. They consist of a distyrylbenzene core substituted by an electron donating group DPA and different EWGs, creating a push-pull system of D-π-A type. The π-system is prolonged by one styryl compared to the previous chapter and substitution by two phenyls is in the middle part of the molecule resulting in 2,5-diphenyl-1,4-distyrylbenzenes (DP-DSB). The acceptor (EWG) groups are

hydrogen (H), methyl (Me), cyano (CN), aldehyde (CHO), and dicyanovinylene (DCV).

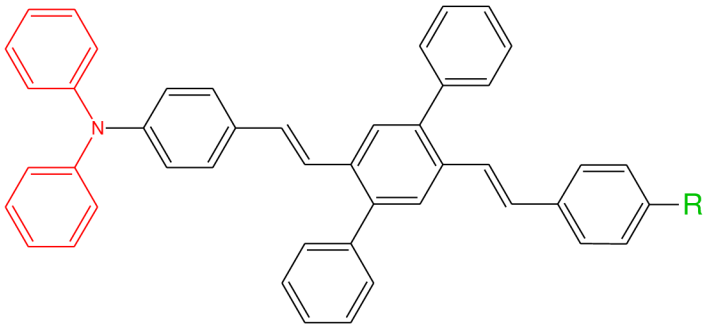

designation	DPA-DP-DSB-H	DPA-DP-DSB-Me	DPA-DP-DSB-CN	DPA-DP-DSB-CHO	DPA-DP-DSB-DCV
R =	−H	$-CH_3$	—CN	−CHO	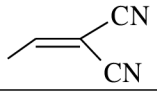

Figure 9 The studied diphenyl-distyrylbenzenes push-pull systems end-capped on one side by diphenylamine (electron donor, red) and on the other by various electron withdrawing groups (green).

4.4.3 Di(thio)ketopyrrolopyrroles

The studied molecules are two relatively well studied derivatives of diketopyrrolopyrrole (DPP) – the DPP is substituted in positions 3 and 6 by either a par of phenyls or a pair of thiophenyls – and their thioketo analogues dithioketopyrrolopyrroles (DTPP).

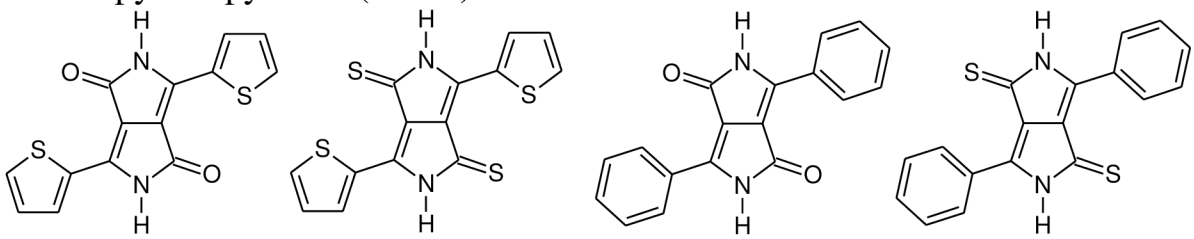

Th-DPP **Th-DTPP** **Ph-DPP** **Ph-DTPP**

Figure 10 Structures of the studied D(T)PP derivatives with designations used in this thesis to address the molecules.

4.4.4 Perovskite materials

The perovskite material used in this work is the well-known methylammonium lead iodide, one of the most studied photovoltaic organic-inorganic hybrid materials. The material was usually used as a mixed halide $MAPbI_{3-x}Cl_x$ precursor, but as our study has shown, the chloride ions content in the resulting crystal structure is negligible. The precursor solutions for the fabrication of thin films were either purchased from Ossila (I101, I201) or prepared from base materials (MAI, PbI_2 and $PbCl_2$) and dissolved in anhydrous dimethylformamide (DMF) with 10 vol % of additive acetyl acetone, all purchased from Sigma-Aldrich.

5 RESULTS OVERVIEW

5.1 Diphenylamino-diphenylstilbenes

5.1.1 Molecular properties

Absorption and fluorescence were studied in three solvents of increasing polarity. Due to their discovered polymorphism (see **5.1.2**), **DPA-DPS-CHO** and **DPA-DPS-DCV** were additionally studied in two more solvents. The solvents used were in order of increasing polarity: toluene, chloroform, (dichloromethane, acetone), and acetonitrile. The molar absorptivities were estimated in all solvents and the values were in the range of 2–4,5 · 10^4 $l \cdot mol^{-1} \cdot cm^{-1}$ (in **Figure 11** the absorptivities in toluene are depicted). The absorption and fluorescence excitation spectra are almost identical for all compounds in all solvents, with no significant differences. The dependence of wavelengths of absorption maxima on solvent polarity is similar to other compounds of D-π-A structure [60–62], i.e. the absorption maxima are not significantly affected by solvents. When comparing the different end-capping groups, we observe a bathochromic shift in order **–V** → **–DBrV** → **–CN** → **–CHO** → **–DCV** indicating their relative accepting strength.

On contrary to the absorption and excitation spectra, the emission is strongly solvent-dependent. Both the wavelengths of the maxima and the shape of the spectra are significantly changing with solvent polarity. The wavelength of emission shows bathochromic shift with increasing solvent polarity. The magnitude of the shift increases with the polarity of the derivative. The shift is accompanied by a redistribution of vibronic intensity from 0-0 vibronic transition (0-1 in case of the **–DCV** derivative) in toluene towards 0-1 and higher vibronic transition in chloroform and more polar solvents respectively.

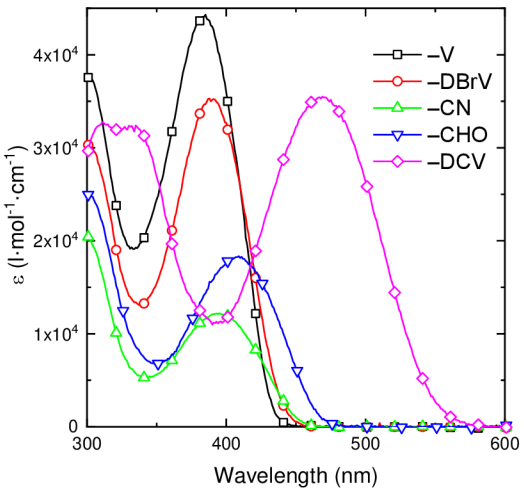

Figure 11 Absorptivities in toluene.

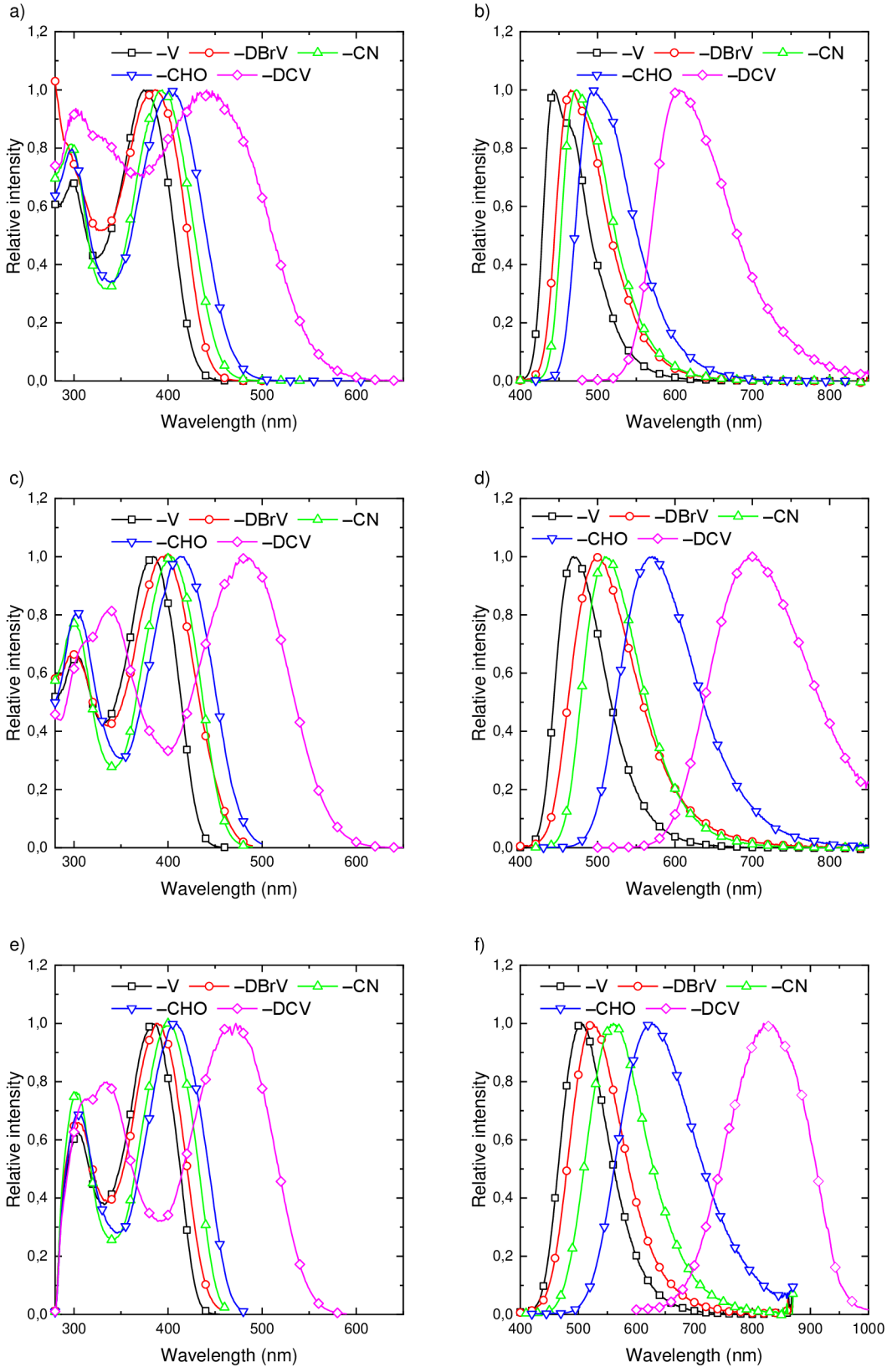

Figure 12 Fluorescence of the studied derivatives in toluene (a, b), chloroform (c, d) and acetonitrile (e,f). The plots a), c) and e) represent excitation spectra, and the plots b), d) and f) represent fluorescence emission spectra. Note the expanded range of wavelengths in plot f).

The two extra solvents in which the most polar derivatives (**–CHO** and **–DCV**) were studied were dichloromethane and acetone, all studied properties follow trends of solvent polarity dependence in these solvents.

To assess the influence of side phenyl substitution, we compare the two more closely inspected compounds **DPA-DPS-CHO** and **DPA-DPS-DCV** with the properties of their earlier published DPA-stilbene-(-CHO / -DCV) counterparts. The **–CHO** derivative shows a similar behaviour in solution as other compounds with DPA-π-CHO [**Chyba! Nenalezen zdroj odkazů.**, 61]. The absorption and luorescence dependence on solvent polarity is quite similar to DPA-biphenyl-CHO [61], i.e. almost no effect on absorption and notable bathochromic shift with increasing polarity, a common feature of D-π-A compounds [60]. In contrast, the spectral as well as photophysical properties of **DPA-DPS-DCV** are notably different from those of DPA-stilbene-DCV [62]. When comparing absorption maxima, we observe considerable red-shift (from 395 to 473 nm and from 394 to 470 nm, respectively). These shifts are even more pronounced for fluorescence maxima (from 524 to 752 nm in dichloromethane and from 488 nm in benzene to 605 nm in toluene). The fluorescence quantum yields of **DPA-DPS-DCV** are higher in less polar solvents than those of DPA-stilbene-DCV. These (dramatic) changes resulting from the decoration of the molecule by side phenyls are exactly opposite to the effect predicted by theoretical calculations based on time-dependent (TD) DFT/DFT. We are unable to satisfactorily explain these slight (**–CHO**) or dramatic (**–DCV**) shifts. We are left only with speculation that correct description of both the absorbing and emitting states of these push–pull stilbenes in solution requires an involvement of charge transfer structures, as in merocyanines [63].

5.1.2 Solid state properties

Due to impurity observed in spectra of **–DCV** in acetonitrile, the synthesis of both the **–DCV** and its key intermediate **–CHO** derivatives was repeated, with an extra purification step, resulting in 2 batches: batch 1 without and batch 2 with further purification. As a result of purification, the impurity emission disappeared and obtained spectra of the studied compounds are shown in the previous chapter. An interesting outcome of the purification was that **DPA-DPS-DCV** crystallized in a new modification showing a more intense and red-shifted SSF. The second batch also produced single crystals suitable for crystal structure determination by single-crystal XRD, see **Figure 14**. Based on different emission wavelengths, the polymorphs of the **–DCV** derivative were denoted **R** (red – batch 1) and **IR** (infrared – batch 2) and the polymorphs of the **–CHO** derivative were denoted **DG** (dark green – batch 1) and **G** (green – batch 2). All five compounds show solid-state fluorescence ranging from blue over green to (infra)red, which was easily detectable by the naked eye. The emission spectra are shown in **Figure 13**.

The moderate fluorescence (Φ_F > 10 %) of the first three compounds is ascribed to an effect of the introduction of side phenyls to push-pull substituted diphenyl-stilbenes. The bulky side phenyls generally disable specific quenching

intermolecular interactions, resulting in molecules showing isolated-like behaviour in crystals. The shape of the fluorescence spectra and the positions of the maxima is similar to the spectra in solution, but we observe a considerable decrease in fluorescence quantum yield, which is expected in polycrystalline materials [64].

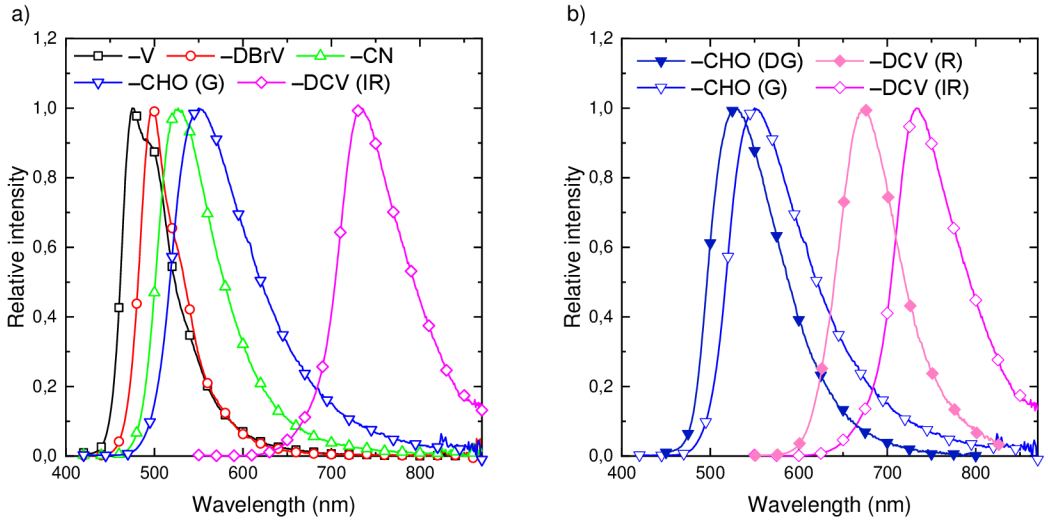

Figure 13 Solid state fluorescence spectra of the studied derivatives (a) and comparison of the SSF of the polymorphs (b).

The fluorescence spectra of both polymorphs of both compounds (**–CHO** and **–DCV**) are shown in **Figure 13b**. The polymorphs of **DPA-DPS-CHO** emit in the green part of the spectrum (maxima: **DG** – 527 nm; **G** – 550 nm) with moderate quantum yields of 10 % (**DG**) and 5 % (**G**). Both polymorphs have a lower fluorescence quantum yield than **–CHO** in any of the studied solutions.

Thus, neither TPA group nor DPS-bridge can be considered as generating aggregation-induced emission. This is not unexpected for the TPA group, but for the DPS bridge, it is a contrary behaviour to the one observed in TPE regioisomer [8].

The polymorphs of **DPA-DPS-DCV** show moderate far-red emission (**R**: 672 nm, 5 %) and stronger infrared emission (**IR**: 733 nm, 32 %). Such parameters are only seldom reported, four-coordinated boron compounds [65] may be stated as one of only few examples. The emission of polymorph **R** comes from an isolated monomer, as is the case of the other studied compounds, while for polymorph **IR**, the emission is considered to be a product of excimer fluorescence of dimer 1 (**Figure 14**).

As a further support of our interpretation of the source of emission, we observe an evident similarity of the crystal structure and spectral and photophysical properties of **R** and **IR** polymorphs to the recently reported cruciform excimer-type emitter abbreviated by authors as DFPA [9].

The stability of polymorphs was confirmed by single-crystal XRD, which showed no considerable changes after several months of storage; the fluorescence of the polycrystalline powder was also well reproducible. On the other hand, when the powder is pressed between two pieces of glass, the fluorescence maximum shows an immediate hypsochromic shift of about 60 nm (from 733 to 670 nm), i.e., near to the

fluorescence maximum of polymorph **R**. The **IR** polymorph can thus be considered as stimuli-responsive.

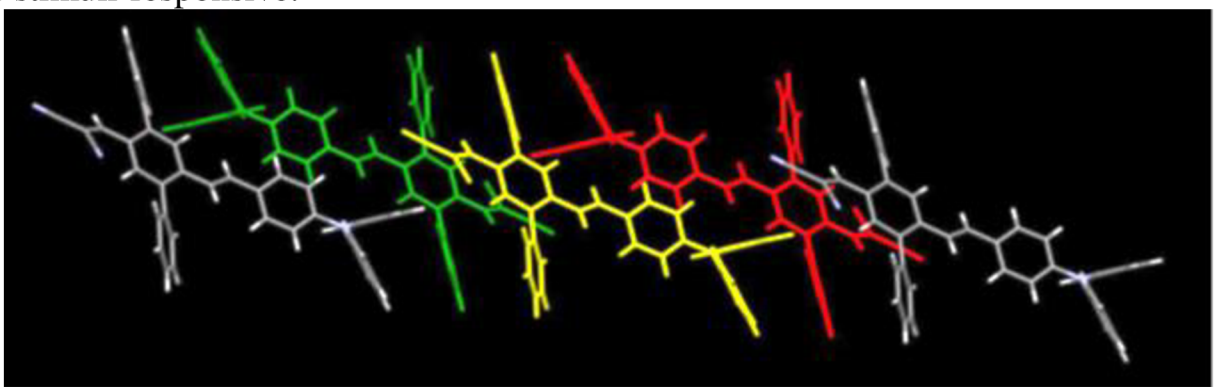

Figure 14 Solid state packing of polymorph **IR**. Highlighted are two alternating dimers: stacked dimer 1: green-yellow (emissive) and unstacked dimer 2: yellow-red (non-emissive). Taken from [66].

5.1.3 Conclusions

In summary, a series of new stilbene-based molecules with different push-pull systems was characterized. The molecules were decorated with side phenyls to affect the packing in the solid state and thus prevent solid-state fluorescence quenching. The investigation of absorption and fluorescence spectra shows that different electron withdrawing groups lead to an expected red shift with increasing electron withdrawing strength. This shift is quite pronounced, up to more than 300 nm in acetonitrile. As is common for molecules with D-π-A structure, the solvatochromism is almost negligible, while we observe a pronounced bathochromic shift of fluorescence with increasing solvent polarity.

The side phenyl substitution, as expected, decreases the interaction in the solid state and promotes efficient SSF (quantum yields over 10 %). Using different electron withdrawing groups, it is possible to cover a large portion of the visible spectrum (emission maxima wavelengths from 475 to 733 nm).

Different polymorphs were observed for two of the studied molecules, with highly interesting results for the **–DCV** derivative. Here, the change in crystal structure leads to efficient excimer-type fluorescence in IR wavelengths (733 nm, 32 %).

5.2 Diphenylamino-diphenyl-distyrylbenzenes

5.2.1 Molecular properties

Absorption and fluorescence excitation and emission spectra were measured in three solvents with increasing polarity: toluene, chloroform and acetonitrile. The absorption and fluorescence excitation spectra are almost identical for all compounds in all solvents. With the notable exception of **DPA-DP-DSB-DCV**, whose absorption in acetonitrile is strongly hypsochromically shifted and resembles that of **–CN** and **–CHO** derivatives. This might hint towards loss of electron withdrawing strength of the –DCV group, e.g. through rotation of the group out of

the molecular plane. Although further experiments are needed to convincingly support this hypothesis. The absorption bands are structureless, giving evidence that some band higher than the 0-0 vibronic transition forms the absolute maximum. Molar absorptivities are ranging from approximately $4 \cdot 10^4$ to $5{,}5 \cdot 10^4$ $l \cdot mol^{-1} \cdot cm^{-1}$ (**Figure 15**), the slightly smaller values for (di)cyano-substituted derivatives may be caused by limited aggregation in $CHCl_3$. The absorption follows expected trend of bathochromic shift with increasing polarity.

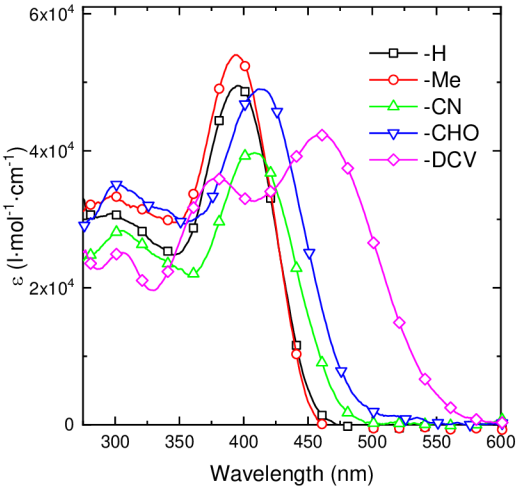

Figure 15 Absorption in chloroform.

On contrary to the absorption and excitation spectra, the emission is strongly solvent-dependent. Both the wavelengths of the maxima and the shape of the spectra are significantly changing with solvent polarity. Both the shape and maxima of the fluorescence emission spectra are considerably different in each solvent (**Figure 2**). The wavelength of emission shows bathochromic shift with increasing solvent polarity. The magnitude of the shift increases with the polarity of the derivative. The shift is accompanied by a change of vibronic intensity from 0-0 vibronic transition (0-1 in case of the –**DCV** derivative) in toluene towards 0-1 and higher vibronic transition in chloroform and more polar solvents respectively. The fluorescence spectra of **–DCV** in acetonitrile correspond to the absorption described above and are comparable to those of compounds without accepting groups (–**H** and –**Me**), suggesting hindered influence of the DCV group also in the excited state. As mentioned above, further experiments are required to corroborate this hypothesis.

In toluene, all compounds exhibit strong fluorescence (Φ_F is over 79 %), in chloroform slight or moderate (–**CHO**) decrease in Φ_F is observed. Similar solvent effect on vibronic intensities was observed for the bis donor (DPA)-substituted DP-DSB [67]. For –**DCV** derivative we observe a dramatic decrease of Φ_F to less than 1%). In acetonitrile the trend observed for the –**H** and –**Me** derivatives continues. In the case of **–CHO** fluorescence, the quantum yield drops below 1 %, similarly to the **–DCV** in chloroform, and a shoulder peak appears at 500 nm.

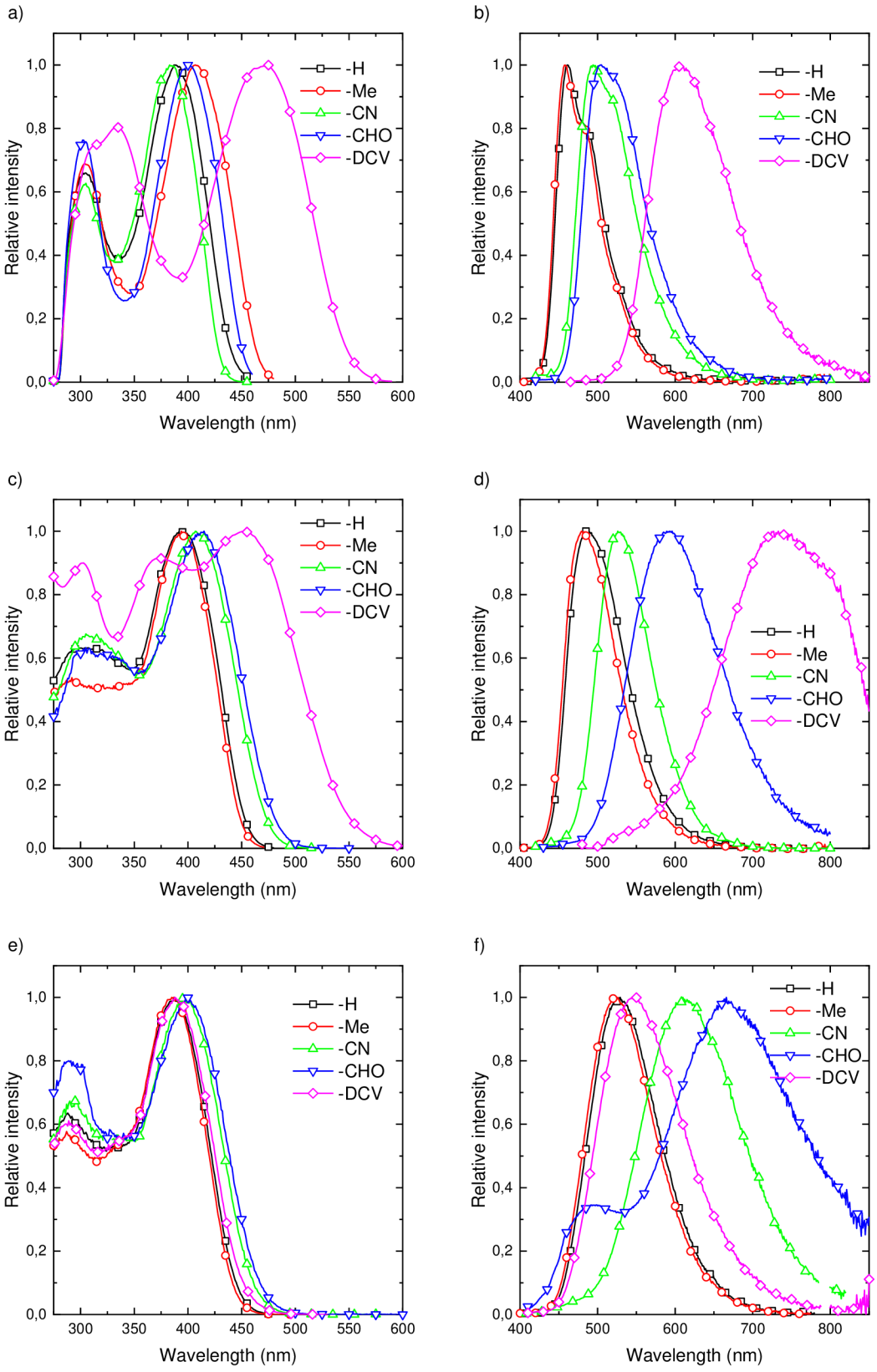

Figure 16 Fluorescence of the studied derivatives in toluene (a, b), chloroform (c, d) and acetonitrile (e,f). The plots a), c) and e) represent excitation spectra, and the plots b), d) and f) represent fluorescence emission spectra.

5.2.2 Solid state properties

The solid state samples were studied in the form of polycrystalline powders. The powders were used as received without any further modification after complete synthesis (including purification). All five compounds under study showed SSF ranging from blue over green to red, which was easily detectable by the naked eye. Their emission spectra are shown in **Figure 17**. The fluorescence is a result of the design principle, i.e. an introduction of side phenyls to push-pull substituted distyrylbenzenes, which generally disables specific quenching intermolecular interactions. Molecules in crystals behave like isolated, as seen from the shape of their spectra and the position of the maxima, which is not far from the spectra in solution.

The quantum yields of SSF are relatively high for **DPA-DP-DSB-Me**, **-CN**, and **-CHO**, considering that polycrystalline materials always produce a decrease in Φ_F with respect to monocrystals, as has been shown for symmetrically substituted DSBs [64]. Although in solution the photophysical properties of **DPA-DP-DSB-H** are almost the same as those of **DPA-DP-DSB-Me**, due to weak electronic effects of the methyl substituent, its SSF characteristics are considerably different. The quantum yield of the former is about half of the latter, and the decay is fitted only by four exponentials with a considerable contribution of extremely short (0,25 ns) and long (17,59 ns) ones. These components may reflect another type of aggregation in the bulk crystal. Thus, it appears that the substitution of both terminal positions of the DSB core is important not only from the electronic point of view, but also from the steric point of view (i.e. disabling too tight packing).

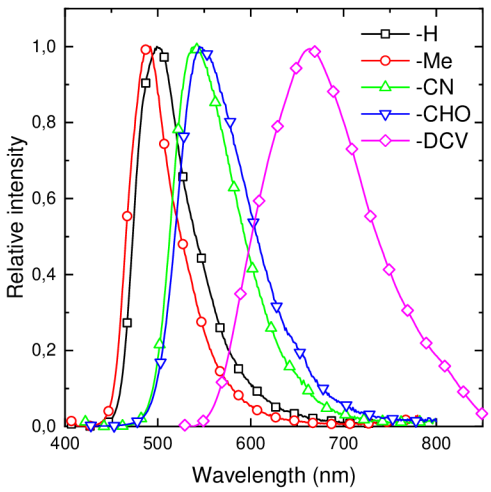

Figure 17 Solid state fluorescence of the studied derivatives.

The expectations put into the synthesis of **DPA-DP-DSB-DCV** were only partially met. This compound emits at a longer wavelength compared to the **DPA–DCV** substituted spirofluorenes [68]. It also behaves like an isolated fluorophore with SSF decay similar to the other three strongly fluorescent DSBs, but its Φ_F is low.

5.2.3 Host-Guest Systems

In an attempt to obtain a strongly emitting system with emission in the red region, promising candidates were selected from the studied compounds to be used in the host-guest arrangement. The idea is to utilize energy transfer from a strongly luminescent molecule to a molecule emitting in the desired region and thus achieve higher photoluminescence quantum yield.

The guest molecule in the system was red-emitting **–DCV** substituted compound. As a suitable host matrix, the **–CN** substituted compound was selected. In the selection process, the overlap of host emission and guest excitation spectra was taken into account. The **–CN**:**–DCV** pair offers great spectral overlap (over 90 %) and high fluorescence quantum yield, while both compounds are structurally similar.

The host-guest systems were prepared in two molar ratios 100:1 and 1000:1. For both molar ratios of the host matrix to the guest molecule, a great increase in fluorescence is observed (from 5 to 20 %). The wavelength of fluorescence maximum is hypsochromically shifted with the decreasing amount of guest molecule. The host fluorescence is well observable in the sample with a lower molar ratio of guest to host (**Figure 18**). The fluorescence decay is fitted by four exponentials, and the fitted decay times increase with decreasing guest ratio.

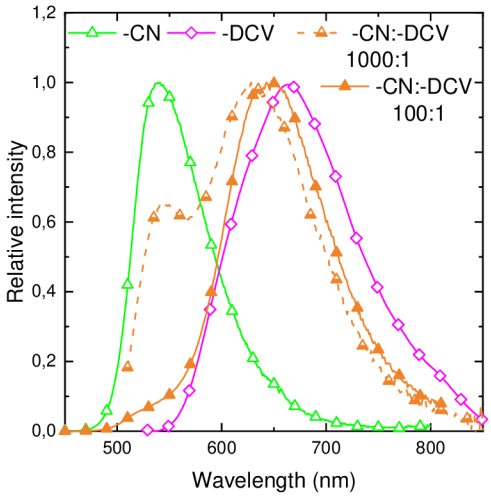

Figure 18 Emission spectra of host and guest compounds and host-guest systems.

5.2.4 Conclusions

A new class of all-*trans* push-pull substituted sterically hindered distyrylbenzenes was studied. All compounds fluoresce strongly in nonpolar solvents. The side phenyls and terminal donor and acceptor substituents of the final distyrylbenzenes disabled a close packing in the condensed phase. As a result, intense solid-state fluorescence, retaining similar character as in solution, was observed in most cases. This fluorescence covers a large region of the visible spectrum (492–652 nm), although the efficiency of red emission is low (~5 %).

The host-guest system approach was used to enhance the red emission and allowed the preparation of polycrystalline material showing strong ($\Phi_F = 20$ %) emission in red spectral region (~645 nm).

The two classes of compounds studied in chapters **5.1** and **5.2** are structurally related and share the structure-properties relationship strategy of utilizing the side phenyls to promote SSF and different EWG end-capping groups to shift the emission colour. It is useful to summarize comparison of molecules with the same or similar (–**V** vs. –**Me**) electron withdrawing groups between the **DPA-DPS-** and **DPA-DP-DSB-** classes. As expected, the larger π-conjugated system of **DPA-DP-DSB-** compounds leads to a narrower bandgap, manifested in longer wavelengths of maxima of both absorption and fluorescence. This is universal across all relevant compound pairs in all solutions and in solid state as well, with the exception of –**DCV** derivatives. From the comparison of PLQY we see that **DPA-DP-DSB-** compounds show overall higher values than their **DPA-DPS-** counterparts, and are also more predictable showing steady decrease with increasing solvent polarity.

The behaviour of the **–DCV** derivatives is rather unexpected. The derivative with a smaller π-conjugated system (**DPA-DPS-DCV**) shows higher wavelength absorption in all cases, but the shift of its emission is hypsochromic (as expected from comparison of size of π-conjugation). The resulting smaller Stokes shift hints towards a smaller effect of solvent relaxation stabilization. This is similar for all of the molecule pairs and might be explained by the difference in the size of molecules.

5.3 Di(thio)ketopyrrolopyrroles

5.3.1 Studied molecules

In the study we compare properties of two DPP molecules and their DTPP counterparts, the molecules under study are: 1,4-diketo-3,6-diphenyl-pyrrolo-[3,4-*c*]-pyrrole (**Ph-DPP**) and 1,4-diketo-3,6-(thiophen-2-yl)-pyrrolo-[3,4-*c*]-pyrrole (**Th-DPP**) and their 1,4-dithioketo heteroanalogues (**Ph-DTPP** and **Th-DTPP**).

The DTPP molecules were synthesized via thionation of the respective DPP by Lawesson's reagent. This one-step synthesis provided relatively high yields (>80 %).

5.3.2 Optical properties

Absorption spectra were measured in DMSO and DMF solutions and solid-state absorption in thin film samples (**Figure 19** and **Table 1**). The spectra in solution in all cases show three vibronic bands with the absolute maximum relating to the 0-0 vibronic transition. Both DTPPs in DMSO exhibit small long-wavelength shoulders. The shifts of the spectral maxima od DPPs are quite clear and expected: the substitution of oxygen by sulphur leads to dramatic red shift (over 100 nm), while replacing of Th- with Ph- causes moderate hypsochromic shift. Compared to the spectra in solution, absorption bands in solid state show similar bathochromic shift. Such behaviour is typical for red-shifted H-aggregates with excitonic coupling [69].

The spectra of DTPPs in thin films are more complex, they are broader and less resolved. Although their absolute maxima have similar bathochromic shifts with respect to those in solution as for DPPs, an additional absorption appears in the long-wavelength region. This absorption takes the form of either a long unresolved tail (**Th-DTPP**), or of a local maximum (**Ph-DTPP**), as has also been found previously [30]. Both DPPs, as is common, exhibit strong fluorescence in solution [70]. However, this fluorescence is completely quenched for DTPPs. All four studied molecules show very weak solid-state fluorescence in thin films.

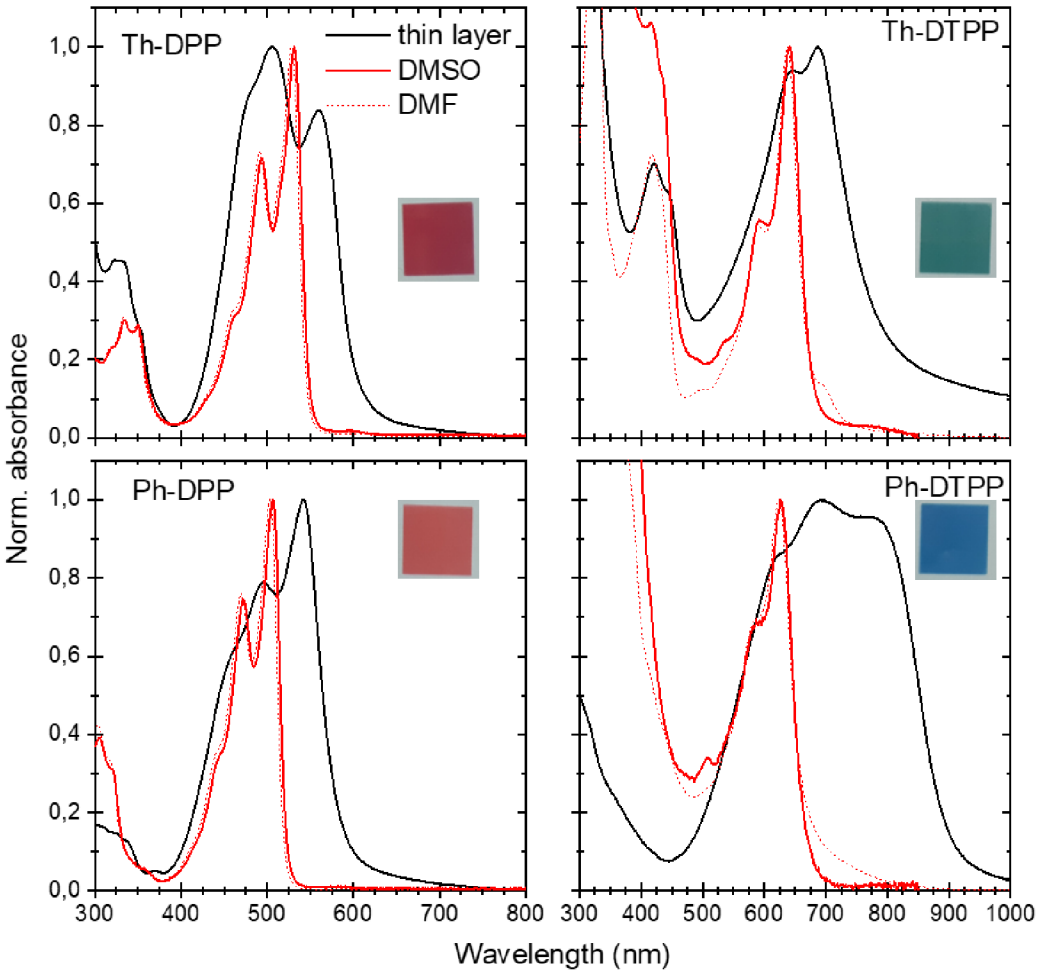

Figure 19 Absorption spectra in DMSO (red), DMF (red dotted) and thin film (black). Photographs of thin films are shown in the insets. Adapted from [71].

To better understand the optical properties and correlate them with X-ray crystal structures, TD DFT calculations were performed by Dr. Luňák. The effect of thionation on the electronic structure of the molecules is as follows. The HOMO level is influenced almost negligibly, the LUMO level is considerably stabilized, and the n-orbital localized on the thioketo group is dramatically destabilized, compared to its energy when localized on the keto group. Consequently, the energies of symmetrically allowed π-π* and n-π* transitions are close, which is crucial for understanding the spectral and photophysical behaviour. The DFT calculations for

DMSO show two allowed spectral transitions in the visible region (π-π* and n-π*) for DTPPs in comparison to one transition (π-π*) for DPPs. This extra transition is then manifested as a long-wavelength shoulder in **Ph-DTPP** and **Th-DTPP** spectra in DMSO. The presence of this nπ* state might be the reason for the absence of fluorescence of both DTPPs in solutions. As has been proved for thionated peryleneimides, thionation leads to an efficient competitive ISC of S(nπ*)→T(ππ*) type [72]. The calculated solid-state absorption spectra based on experimentally found geometry are in good agreement with experimental results. The spectrum of **Th-DTPP** is strongly affected by the n-π* transition, which is also responsible for a long wavelength tailing. The the long wavelength shoulder in the spectrum of **Ph-DTPP** is a product of n-π* transition. This work and calculations helped to elucidate the underlying electronic structure behind the solid-state absorption changes described earlier by J. Mizuguchi [30].

Table 1 Wavelengths of absorption maxima (in nm) in thin layer, DMSO and DMF solutions. For **Th-DPP** the position of 0-0 transition local maximum is added. Fluorescence maxima (PL) in thin film.

Compound	thin layer	DMSO	DMF	PL
Th-DPP	506; 560	531	528	706
Th-DTPP	687	641	638	785
Ph-DPP	542	506	503	624
Ph-DTPP	696	626	624	873

5.3.3 Electrochemical, field-effect mobility, and AFM investigation

Electrochemistry

All DPPs and DTPPs exhibited both oxidation and reduction peaks within the studied potential window. However, their re-oxidation and re-reduction currents were substantially low, since the oxidized and reduced forms were soluble in the electrolyte, indicating irreversible behaviour. The values of E_{HOMO} (resp. E_{LUMO}) were calculated from the oxidation (reduction) onsets using an internal standard (see **4.2**). The values of E_{HOMO}, E_{LUMO} and bandgap energy (E_{gap}) obtained by electrochemical and optical measurements are summarized in **Table 2**. As a result of thionation, DTPP derivatives show an increase in E_{HOMO} and a decrease in E_{LUMO}, resulting in a smaller E_{gap} of 1,1–1,2 eV. The theoretically predicted trend of the effect of thionation, stabilization of LUMO, destabilization of HOMO, was qualitatively confirmed. The stabilization of LUMO resulting from thionation is in accordance with observation and theory (~ 0,5 eV). However, the experimental HOMO destabilization (0,4–0,5 eV) is much higher than predicted (< 0,1 eV). The resulting electrochemical bandgap is considerably lower in comparison to both the

theoretically predicted and experimentally determined ones. An interface barrier between the electrode surface and the solution is the most probable cause.

Table 2 E_{HOMO}, E_{LUMO} and E_{gap} obtained by electrochemical measurements and E_{gap} obtained by optical measurements.

Compound	E_{HOMO} (eV)	E_{LUMO} (eV)	E_{gap} (eV) (CV estimate)	E_{gap} (eV) (optical)
Th-DPP	−6,0	−3,9	2,1	2,0
Th-DTPP	−5,6	−4,5	1,1	1,5
Ph-DPP	−6,2	−4,1	2,1	2,1
Ph-DTPP	−5,7	−4,5	1,2	1,4

Field-effect mobilities

The investigation of the effect of thionation on charge transport was performed by characterizing OFETs with the studied materials as active layer in the device structures. The transfer curves of all materials in Al source-drain contacts transistors, with the exception of **Th-DPP**, show n-type transport with field-effect electron mobilities of 10^{-3}–10^{-2} cm^2/Vs. The **Th-DPP** exhibits poor n-type behaviour with of about 10^{-5} cm^2/Vs. The effect of thionation can be observed from the electron mobility values of both DTPPs being higher than those of **Ph-DPP**. The Au source-drain contacts transistors exhibit field-effect hole mobilities $\approx 10^{-3}$ cm^2/Vs for the DPP materials, while the values for **Th-DTPP** and **Ph-DTPP** were one order of magnitude lower ($\approx 10^{-4}$). All the OFET characteristic values are summarized in **Table 3**.

Table 3 Field effect mobilities, threshold voltages and on/off ratio values of studied materials in OFETs with n-type (Al) and p-type (Au) enhancing configurations.

contact material		Th-DPP	Th-DTPP	Ph-DPP	Ph-DTPP
Al	μ_e ($cm^2 \cdot V^{-1} \cdot s^{-1}$)	$1{,}2 \cdot 10^{-5}$	$7{,}4 \cdot 10^{-3}$	$2{,}7 \cdot 10^{-3}$	$1{,}8 \cdot 10^{-2}$
Au	μ_h ($cm^2 \cdot V^{-1} \cdot s^{-1}$)	$2{,}0 \cdot 10^{-3}$	$4{,}9 \cdot 10^{-4}$	$6{,}6 \cdot 10^{-3}$	$3{,}0 \cdot 10^{-4}$
Al	V_{th} (V)	12,2	4,4	3,2	4,1
Au	V_{th} (V)	−3,7	−5,9	−6,0	−10,6
Al	on/off ratio	$\sim 10^2$	$\sim 10^3$	$\sim 10^3$	$\sim 10^4$
Au	on/off ratio	$\sim 10^3$	$\sim 10^2$	$\sim 10^3$	$\sim 10^1$

The effect of thionation is a substantial increase of the n-type mobility with simultaneous decrease of the p-type mobility, resulting in the change of a p-type semiconductor (**Th-DPP**) or an ambipolar semiconductor (**Ph-DPP**) to an n-type one. This might be a result of one, the herringbone packing pattern promoted by

thionation, and two, depletion of electron density in parts of the molecule resulting from higher electronegativity of introduced sulphur atoms.

5.3.4 Conclusion

The thionation of diketopyrrolopyrrole pigments affects the molecular structure as well as the solid-state packing. This is reflected in the electronic structure and optical and semiconducting properties. Dithioketopyrrolopyrrole pigments remain thermally stable because of the strong hydrogen bonding. The aryl twists in the molecular structure of DTPPs are more common than those in their DPP counterparts and the molecular structure (along with the properties) is thus affected by crystal packing. In the electronic structure, the characteristic features are the low-lying LUMO and high-lying n-orbital (located on the thioketo group). These features determine the spectral and photophysical properties. The solid-state absorption edge is shifted to the near-infrared and the fluorescence in solution is quenched. As is observed from field-effect experiments, thionation switches p-type/ambipolar DPP semiconductors to n-type DTPP semiconductors. Altogether, DTPPs can be considered as potential electron-accepting components in photovoltaics because of their FR/NIR absorption, low-lying LUMO, and n-type mobility.

5.4 Perovskite materials for photonic applications

5.4.1 Stability of hybrid perovskite layer

To examine the effect of moisture on the active part of the perovskite solar cells, samples of perovskite layers were placed in a climate chamber with a set humidity of 60 % RH and temperature $\vartheta = 25$ °C for 48 hours. The perovskite layers were then examined by XRD. The measurements were carried out by Dr. Chladil (FME, BUT). The quantitative result of the perovskite and lead iodide content evolution during ageing in the climatic chamber is listed in **Table 4** in the form of molar percentage. The results revealed that in the case of the as-prepared sample the PbI_2 content was over 8 mol%. During the first 24 hours of ageing the perovskite structure lost more than 5,5 mol% and during the next 24 hours it lost even more than 16 mol%. The speed of perovskite degradation to lead iodide appears to increase with time.

Table 4 Evolution of perovskite and lead iodide content in the perovskite layer during ageing

	As prepared	**24 hours**	**48 hours**
PbI_2 (mol%)	8,3	14,0	30,3
$MAPbI_3$ (mol%)	91,7	86,0	69,7

Our study of perovskite layers has also shown the important role of atmospheric moisture during the formation of the perovskite layer. We have found that films manufactured in atmosphere with 15% RH have different structure to those manufactured in dry nitrogen atmosphere of glovebox. This is well observable by

atomic force microscopy (AFM) imaging of the layer topography The perovskite active layer created in an inert atmosphere has a less continuous morphology. After moisture exposure of both samples in the climate chamber with 60% RH for 48 hours, the perovskite grains merged, leading to an enlargement of their volume. The merging of the grains led to clustering and the gaps between the grains have spread as a result. Such an increase in recombination centers along with PbI_2 increase (**Table 4**) causes drop in conversion efficiency. From the AFM measurements, it is also evident that the perovskite layer in which the moisture was present during the manufacturing process tends to form larger grains. However, this assumption would be better to confirm with further investigation in follow-up research.

5.4.2 The influence of active layer degradation on solar cell device

In order to analyse the effects causing degradation of the perovskite active layer in photovoltaic cells, two series of perovskite solar cells were manufactured. The fabrication of photovoltaic cell series differed in the environment in which they were manufactured. In the first series, nine samples were fabricated in a glovebox with a nitrogen atmosphere with a negligible moisture content (< 1 ppm). In the second series, six samples were fabricated in a dry air box with controlled humidity set to a value of 15% RH. **Table 5** shows the averaged parameters of cells from both series, the uncertainties were established as sample standard deviation of all working cells of all samples in each of the series.

Table 5 Parameters of the perovskite solar cells manufactured in dry nitrogen and 15% RH air atmospheres.

Series	j_{sc} (mA/cm^2)	V_{oc} (mV)	P_{max} (mW)	***FF*** (%)	η (%)
1 (N2)	17,7 ± 0,8	899± 20	0,5± 0,1	65± 2	10,4± 0,9
2 (15% RH air)	17,4 ± 1,7	892 ± 17	0,25 ± 0,05	33 ± 3	5,2 ± 0,6

The perovskite solar cells from the first series had very good results in terms of conversion efficiency (record cell: η = 11,9 %, FF = 69 %.), while the cells from the second seriesseries perovskites cells were noticeably worse. In the second series, the record cell showed only η = 6,2 % and FF = 37 %. It can be seen that the j_{sc} and V_{oc} parameters are comparable in both series, but there is considerable decrease of FF in series 2. This drop may be caused by the use of a different perovskite solution designed for air processing. However, for the purpose of investigating degradation, these values were sufficient.

The samples from both series were stored for the same time in a climate chamber in pairs of one cell from each series. The current-voltage characteristics were measured in a 24-hour interval with increasing relative humidity and a constant temperature of 25 °C. The first series solar cells had a significant drop in performance after the relative humidity in the chamber has exceeded 50% RH. At 60% RH, the short-circuit current has seriously dropped, with even further drop accompanied by decrease of open-circuit voltage at 70% RH. After this, the cells

became almost inactive. Despite the considerably worse parameters, the solar cells from the second series are more resistant against external moisture degradation. Above the 50% RH limit, their performance started to diminish, but not on such a scale as the cells from the first series. As in the first case, the main effect has been the decrease of short-circuit current. The manufacturing process carried out in an air atmosphere with 15% relative humidity has therefore proved to be more advantageous for perovskite solar cells. The explanation may be that the perovskite structures produced in the 15% RH environment form more uniform structure with fewer grain boundaries may be the cause of increased resistance to the permeation of water molecules into perovskite crystals and its subsequent disruption [73].

5.4.3 Addition of auxiliary layer into the PSC structure

An organic semiconducting pigment, which will serve as a charge transporting layer (due to its semiconducting nature) as well as a passivation layer (due to its hydrophobicity) is tested to increase the stability and performance of PSC. The proposed materials were phenyl and thiophenyl derivatives of dithioketo-pyrrolopyrrole (**Th-DTPP** and **Ph-DTPP**). The materials were selected based on their advantageous position of energy levels and field effect mobilities and strongly preferred n-type transport. Electron mobilities reached sufficient values (over $1 \cdot 10^{-3}$ $cm^2V^{-1}s^{-1}$), for comparison, one of the most widely used electron transporting materials, PCBM, is reported to show electron field-effect mobility in the order of $10^{-3} – 10^{-2}$ $cm^2V^{-1}s^{-1}$ [74].

The materials were tested as passivation and transporting layer in a series of solar cells. Cells were constructed with an inverted structure with the addition of PVD step to introduce **Th-DTPP** on top of $PC_{60}BM$.

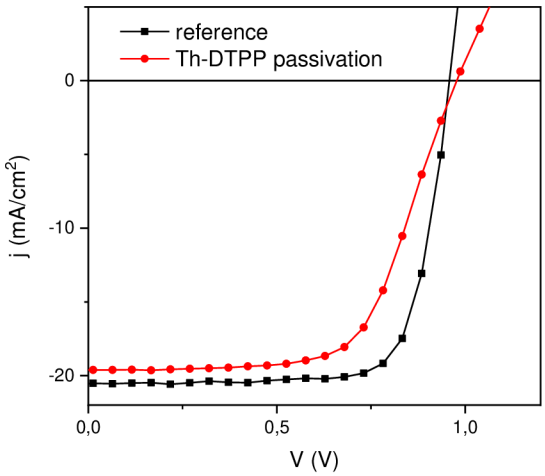

Figure 20 I-V curves or representative cells – reference (black) and Th-DTPP passivated (red).

The representative I-V curves for experimental cells and reference cells are shown in **Figure 20**. As can be seen from the shape of the red curve, the **Th-DTPP** passivation layer increases the contact resistance. On the other hand, we see a slight

increase in V_{oc} hinting towards lower barriers at electrode contact [75]. The average parameters of all cells are summarized in **Table 6**. We can see that the introduction of the passivation layer had only a slight diminishing effect on the performance of the cells (in contrast to OA). As for increase in cell stability, the relative values of parameters are shown in **Table 7**.

Table 6 Parameters of reference and Th-DTPP passivated perovskite solar cells.

	j_{sc} (mA/cm^2)	V_{oc} (mV)	*FF* (%)	η (%)
reference	20 ± 1	960 ± 10	66 ± 3	13 ± 1
passivated	21 ± 2	972 ± 7	55 ± 5	11 ± 1

Table 7 Relative values of cells' parameters after 2 weeks ageing in ambient environment.

Relative value afte 2 weeks	j_{sc}	V_{oc}	*FF*	η
reference (%)	101	102	88	90
passivated (%)	97	100	83	81

The results of stability study show that the main reason for decreasing efficiency is the decline in the fill factor. We also see that the power conversion efficiency of the passivated cells dropped more than that of the references. This could be the result of prolonged exposure to air and increased stress of the active layer during the deposition of passivating pigment. Nevertheless, the results have shown that a double purpose pigment layer is a possible way to improve the performance of PSCs, although more experiments and optimization is necessary. A more thorough stability study is one of the plans for the future work.

5.4.4 Conclusions

The research of utilization of organic semiconductor materials in perovskite solar cells has yielded some interesting results and helped us to create a knowledge base for further experiments. First, the conducted stability study has shown the effect of moisture on the stability of perovskite layers and solar cells and has provided a reference point to which further experiments can be compared. An approach utilizing organic pigments with semiconducting properties as a double-purpose passivation and a charge transport layer has shown promising results. A pigment tested in the study was DTPP material described in the previous chapter of this thesis. It is reasonable to believe that further investigation and optimization of the fabrication process may yield fruitful results.

6 CONCLUSIONS

The aim of this thesis was to study the relationship between the structure and properties of novel organic compounds and their potential utilization in optical and optoelectronic applications. The studied materials were π-conjugated molecules based on stilbene or distyrylbenzene core intended as solid-state fluorophores, and diketopyrrolopyrrole (DPP) semiconductor derivatives for use in organic electronics (mainly photovoltaics). The thesis also focused on work with perovskite materials – one of the leading topics in today's advanced photovoltaics – with the focus on understanding and improving its stability by the means of the utilization of the organic materials studied in our research.

The properties of materials were investigated in solutions, to characterize their fundamental properties as single molecules, and in solid state samples (powders or thin films), to see how the single molecule properties translate to condensed phase and to study the properties in conditions close to the ones in applications.

The π-conjugated stilbene and distyrylbenzene materials were thoroughly studied from the point of view of optical properties. Base structures were substituted by varying electron withdrawing groups to produce two series of molecules with a push-pull system. To prevent interaction in the solid state and promote solid state fluorescence, the molecules were decorated with bulky side phenyl groups. Because of the varying push-pull system, both series of molecules showed fluorescence that covered a large part of the visible spectrum depending on the strength of the push-pull system. The intended effect of side phenyls was achieved and the materials maintained their fluorescent properties almost unchanged in the solid state. Fluorescence ranged from blue to far red (~450–650 nm) with satisfactory fluorescence quantum yield (PLQY > 10 %). Only the PLQY of the distyrylbenzene-based red emitter was lower. However, it can be increased with only minimal hypsochromic shift (~5 nm) using the host-quest system, where a small amount of the red emitter is mixed with other more efficient emitter from this series (in ratio ~1:100). Interesting properties were observed for the red-emitting molecule from the stilbene-based series. This molecule forms an excimer-emitting polymorph with impressive infrared fluorescence (733 nm, 32% PLQY). The significance of the results lies in the presentation of first highly efficient IR emitter and second two series of solid-state emitters with a similar structure that covers a large part of the visible spectrum, thus enabling fine-tuned colour of emission by their mixing. The findings regarding the polymorph emission have been published and the rest of obtained results is in the process of publication as follow up papers.

The studied novel DPP derivatives were thionated forms (DTPP) and objective of the study was to assess the influence of the thionation on optical and electrical properties. It was discovered, that with accordance to literature, the thionation stabilizes LUMO level and subsequently leads to bathochromic shift in emission. These results were correlated with crystallographic structure and theoretical

modelling. For the first time, the influence of thionation on electrical properties of such materials was observed. The results show a significant shift of thionated materials towards n-type behaviour. Field-effect electron mobilities satisfactory for use in organic photovoltaics (~10^{-2} cm^2/ Vs) and impressively low lying LUMO levels (~ −4,5 eV) were observed for the studied DTPP molecules. All of these results have been published.

The investigation of hybrid materials consisted of a stability study of perovskite material and photovoltaic devices and of testing of approaches to increase the moisture resistance of the hybrid solar cells. The stability study helped to establish a reference point for further research in this area and also showed a beneficial effect of mixed-halide perovskite precursors. The results were successively published in form of conference papers. The experiments with use of the DTPP pigment as passivating/charge transporting layer yielded encouraging results. With further optimization of the fabrication process, the dual-purpose pigment layer approach may lead to better stability of perovskite solar cells.

To conclude, the thesis helped to expand the knowledge base of structure-properties relations to help better design molecules with desired properties. Interesting properties were discovered in some of the studied materials, and the results have been published or are in the publishing process.

7 REFERENCES

1 VARUGHESE, Sunil. Non-covalent routes to tune the optical properties of molecular materials. *Journal of Materials Chemistry C*. 2014, **2**(18). ISSN 2050-7526. DOI:10.1039/c3tc32414a

2 BERA, Manas Kumar, Prasanta PAL a Sudip MALIK. Solid-state emissive organic chromophores: design, strategy and building blocks. *Journal of Materials Chemistry C*. 2020, **8**(3), 788-802. ISSN 2050-7526. DOI:10.1039/C9TC04239C

3 YUAN, Kang, Xiang WANG, Soren K MELLERUP, Igor KOZIN a Suning WANG. Spiro-BODIPYs with a Diaryl Chelate: Impact on Aggregation and Luminescence. *The Journal of Organic Chemistry*. 2017, **82**(24), 13481-13487. ISSN 0022-3263. DOI:10.1021/acs.joc.7b02602

4 KU, Sung-Yu, Liang-Chen CHI, Wen-Yi HUNG, Shih-Wei YANG, Tsung-Cheng TSAI, Ken-Tsung WONG, Yu-Hung CHEN a Chih-I WU. High-luminescence non-doped green OLEDs based on a 9,9-diarylfluorene-terminated 2,1,3-benzothiadiazole derivative. *J. Mater. Chem.* 2009, **19**(6), 773-780. ISSN 0959-9428. DOI:10.1039/B814082K

5 ZHAO, Qiuli a Jing Zhi SUN. Red and near infrared emission materials with AIE characteristics. *Journal of Materials Chemistry C*. 2016, **4**(45), 10588-10609. ISSN 2050-7526. DOI:10.1039/C6TC03359H

6 SHIMIZU, Masaki a Tamejiro HIYAMA. Organic Fluorophores Exhibiting Highly Efficient Photoluminescence in the Solid State. *Chemistry - An Asian Journal*. 2010, **5**(7), 1516-1531. ISSN 18614728. DOI:10.1002/asia.200900727

7 SHIMIZU, Masaki, Rina KAKI, Youhei TAKEDA, Tamejiro HIYAMA, Naomi NAGAI, Hideo YAMAGISHI a Hiroyuki FURUTANI. 1,4-Bis(diarylamino)-2,5-bis(4-cyanophenylethenyl)benzenes: Fluorophores Exhibiting Efficient Red and Near-Infrared Emissions in Solid State. *Angewandte Chemie International Edition*. 2012, **51**(17), 4095-4099. ISSN 14337851. DOI:10.1002/anie.201108943

8 MEI, Ju, Nelson L. C. LEUNG, Ryan T. K. KWOK, Jacky W. Y. LAM a Ben Zhong TANG. Aggregation-Induced Emission: Together We Shine, United We Soar!. *Chemical Reviews*. 2015, **115**(21), 11718-11940. ISSN 0009-2665. DOI:10.1021/acs.chemrev.5b00263

9 ZHANG, Yujian, Jianxu ZHANG, Jiahao SHEN, Jingwei SUN, Kai WANG, Zhigang XIE, Huiwen GAO a Bo ZOU. Solid-State TICT-Emissive Cruciform: Aggregation-Enhanced Emission, Deep-Red to Near-Infrared Piezochromism and Imaging In Vivo. *Advanced Optical Materials*. 2018, **6**(22). ISSN 21951071. DOI:10.1002/adom.201800956

10 FARNUM, Donald G., Goverdhan MEHTA, George G.I. MOORE a Frederick P. SIEGAL. Attempted reformatskii reaction of benzonitrile, 1,4-diketo-3,6-diphenylpyrrolo[3,4-C]pyrrole. A lactam analogue of pentalene. *Tetrahedron Letters*. 1974, **15**(29), 2549-2552. ISSN 00404039. DOI:10.1016/S0040-4039(01)93202-2

11 POTRAWA, Thomas a Heinz LANGHALS. Fluoreszenzfarbstoffe mit großen Stokes-Shifts – lösliche Dihydropyrrolopyrroldione. *Chemische Berichte*. 1987, **120**(7), 1075-1078. ISSN 0009-2940. DOI:10.1002/cber.19871200702

12 VALA, Martin, Martin WEITER, Jan VYŇUCHAL, Petr TOMAN a Stanislav LUŇÁK. Comparative Studies of Diphenyl-Diketo-Pyrrolopyrrole Derivatives for Electroluminescence Applications. *Journal of Fluorescence*. 2008, **18**(6). ISSN 1053-0509. DOI:10.1007/s10895-008-0370-x

13 DHAR, Joydeep, Durga Prasad KAROTHU a Satish PATIL. *Herringbone to cofacial solid state packing via H-bonding in diketopyrrolopyrrole (DPP) based molecular crystals: influence on charge transport*. 97-100. DOI:10.1039/C4CC06063F

14 KOVALENKO, Alexander, Cigdem YUMUSAK, Patricie HEINRICHOVA, et al. Adamantane substitutions: a path to high-performing, soluble, versatile and sustainable organic semiconducting materials. *Journal of Materials Chemistry C*. 2017, **5**(19), 4716-4723. ISSN 2050-7526. DOI:10.1039/C6TC05076J

15 YANG, Jie, Hanlin WANG, Jinyang CHEN, et al. Bis-Diketopyrrolopyrrole Moiety as a Promising Building Block to Enable Balanced Ambipolar Polymers for Flexible Transistors. *Advanced Materials*. 2017, **29**(22). ISSN 09359648. DOI:10.1002/adma.201606162

16 HUO, Lijun, Jianhui HOU, Hsiang-Yu CHEN, Shaoqing ZHANG, Yang JIANG, Teresa L. CHEN a Yang YANG. Bandgap and Molecular Level Control of the Low-Bandgap Polymers Based on 3,6-Dithiophen-2-yl-2,5-dihydropyrrolo[3,4- c]pyrrole-1,4-dione toward Highly Efficient Polymer Solar Cells. *Macromolecules*. 2009, **42**(17), 6564-6571. ISSN 0024-9297. DOI:10.1021/ma9012972

17 BEYERLEIN, Thomas, Bernd TIEKE, Stefan FORERO-LENGER a Wolfgang BRÜTTING. Red electroluminescence from a 1,4-diketopyrrolo[3,4-c]pyrrole (DPP)-based conjugated polymer. *Synthetic Metals*. 2002, **130**(2), 115-119. ISSN 03796779. DOI:10.1016/S0379-6779(02)00058-9

18 QU, Yi, Jianli HUA a He TIAN. Colorimetric and Ratiometric Red Fluorescent Chemosensor for Fluoride Ion Based on Diketopyrrolopyrrole. *Organic Letters*. 2010, **12**(15), 3320-3323. ISSN 1523-7060. DOI:10.1021/ol101081m

19 FUKUDA, M. Evaluation of new organic pigments as laser-active media for a solid-state dye laser. *Dyes and Pigments*. 2004, **63**(2), 115-125. ISSN 01437208. DOI:10.1016/S0143-7208(04)00013-0

20 GRZYBOWSKI, Marek, Vincent HUGUES, Mireille BLANCHARD-DESCE a Daniel T. GRYKO. Two-Photon-Induced Fluorescence in New π-Expanded Diketopyrrolopyrroles. *Chemistry - A European Journal*. 2014, **20**(39), 12493-12501. ISSN 09476539. DOI:10.1002/chem.201402569

21 YANAGISAWA, Hiroyuki, Jin MIZUGUCHI, Shinji ARAMAKI a Yoshimasa SAKAI. Organic Field-Effect Transistor Devices Based on Latent Pigments of Unsubstituted Diketopyrrolopyrrole or Quinacridone. *Japanese Journal of Applied Physics*. 2008, **47**(6), 4728-4731. ISSN 0021-4922. DOI:10.1143/JJAP.47.4728

22 GŁOWACKI, Eric Daniel, Halime COSKUN, Martin A. BLOOD-FORSYTHE, et al. Hydrogen-bonded diketopyrrolopyrrole (DPP) pigments as organic semiconductors. *Organic Electronics*. 2014, **15**(12), 3521-3528. ISSN 15661199. DOI:10.1016/j.orgel.2014.09.038

23 RASOOL, Shafket, Quoc Viet HOANG, Doan Van VU, et al. High-efficiency single and tandem fullerene solar cells with asymmetric monofluorinated diketopyrrolopyrrole-based polymer. *Journal of Energy Chemistry*. 2022, **64**, 236-245. ISSN 20954956. DOI:10.1016/j.jechem.2021.04.032

24 RYAN, James W. a Yutaka MATSUO. Increased Efficiency in Small Molecule Organic Solar Cells Through the Use of a 56-π Electron Acceptor – Methano Indene Fullerene. *Scientific Reports*. 2015, **5**(1). ISSN 2045-2322. DOI:10.1038/srep08319

25 ZHANG, Yuan, Xuan-Dung DANG, Chunki KIM a Thuc-Quyen NGUYEN. Effect of Charge Recombination on the Fill Factor of Small Molecule Bulk Heterojunction Solar Cells. *Advanced Energy Materials*. 2011, **1**(4), 610-617. ISSN 16146832. DOI:10.1002/aenm.201100040

26 PRIVADO, María, Virginia CUESTA, Pilar DE LA CRUZ, Mukhamed L. KESHTOV, Ganesh D. SHARMA a Fernando LANGA. Tuning the optoelectronic properties for high-efficiency (>7.5%) all small molecule and fullerene-free solar cells. *Journal of Materials Chemistry A*. 2017, **5**(27), 14259-14269. ISSN 2050-7488. DOI:10.1039/C7TA03815A

27 ROCHAT, Alain Claude, Abul IQBAL, Rémy JEANNERET a Jin MIZUGUCHI. *Dithioketo-pyrrolo-pyrroles, process for their preparation and use*. 1985. EP0187620. Filed 1985.

28 CLOSS, Fritz a Rudolf GOMPPER. 2,5-Diazapentalene. *Angewandte Chemie*. 1987, **99**(6), 566-567. ISSN 00448249. DOI:10.1002/ange.19870990611

29 MIZUGUCHI, Jin a Alain Claude ROCHAT. A New Near-Infrared Photodetector Based on 1,4-Dithioketo-3,6-Diphenyl-Pyrrolo-[3,4-c]-Pyrrole. *Journal of Imaging Science*. 1988, **32**(3), 135-140.

30 MIZUGUCHI, Jin, Alain Claude ROCHAT a Grety RIHS. Electronic Properties of 1,4-Dithioketo-3,6-Diphenyl-Pyrrolo-[3,4-c]-Pyrrole in Solution and in the Solid State. *Berichte der Bunsengesellschaft für physikalische Chemie*. 1992, **96**(4), 607-619. ISSN 00059021. DOI:10.1002/bbpc.19920960415

31 MIZUGUCHI, Jin, Gérald GILLER a Erwin BAERISWYL. Phase change of 1,4-dithioketo-3,6-diphenyl-pyrrolo-[3,4- c]-pyrrole for information storage applications. *Journal of Applied Physics*. 1994, **75**(1), 514-518. ISSN 0021-8979. DOI:10.1063/1.355831

32 QIAN, Gang, Ji QI, James A. DAVEY, James S. WRIGHT a Zhi Yuan WANG. Family of Diazapentalene Chromophores and Narrow-Band-Gap Polymers: Synthesis, Halochromism, Halofluorism, and Visible–Near Infrared Photodetectivity. *Chemistry of Materials*. 2012, **24**(12), 2364-2372. ISSN 0897-4756. DOI:10.1021/cm300938s

33 QIAN, Gang a Zhi Yuan WANG. Near-Infrared Thermochromic Diazapentalene Dyes. *Advanced Materials*. 2012, **24**(12), 1582-1588. ISSN 09359648. DOI:10.1002/adma.201104711

34 RIPAUD, Emilie, Dora DEMETER, Théodulf ROUSSEAU, Emmanuel BOUCARD-CÉTOL, Magali ALLAIN, Riccardo PO, Philippe LERICHE a Jean RONCALI. Structure–properties relationships in conjugated molecules based on diketopyrrolopyrrole for organic photovoltaics. *Dyes and Pigments*. 2012, **95**(1), 126-133. ISSN 01437208. DOI:10.1016/j.dyepig.2012.03.021

35 QIAN, Gang, Ji QI a Zhi Yuan WANG. Synthesis and study of low-bandgap polymers containing the diazapentalene and diketopyrrolopyrrole chromophores for potential use in solar cells and near-infrared photodetectors. *Journal of Materials Chemistry*. 2012, **22**(25), 12867-12873. ISSN 0959-9428. DOI:10.1039/c2jm30868a

36 LÉVESQUE, Simon, David GENDRON, Nicolas BÉRUBÉ, François GRENIER, Mario LECLERC a Michel CÔTÉ. Thiocarbonyl Substitution in 1,4-Dithioketopyrrolopyrrole and Thienopyrroledithione Derivatives: An Experimental and Theoretical Study. *The Journal of Physical Chemistry C*. 2014, **118**(8), 3953-3959. ISSN 1932-7447. DOI:10.1021/jp411300h

37 ZHANG, Haichang, Maning LIU, Wenjun YANG, Lauri JUDIN, Terttu I. HUKKA, Arri PRIIMAGI, Zhifeng DENG a Paola VIVO. Thionation Enhances the Performance of Polymeric Dopant-Free Hole-Transporting Materials for Perovskite Solar Cells. *Advanced Materials Interfaces*. 2019, **6**(18). ISSN 2196-7350. DOI:10.1002/admi.201901036

38 ZHANG, Haichang, Kun YANG, Kai ZHANG, Zhenzhen ZHANG, Qikun SUN a Wenjun YANG. Thionating iso-diketopyrrolopyrrole-based polymers: from p-type to ambipolar field effect transistors with enhanced charge mobility. *Polymer Chemistry*. 2018, **9**(14), 1807-1814. ISSN 1759-9954. DOI:10.1039/C8PY00292D

39 MOMMA, Koichi a Fujio IZUMI. VESTA 3 for three-dimensional visualization of crystal, volumetric and morphology data. *Journal of Applied Crystallography*. 2011, **44**(6), 1272-1276. ISSN 0021-8898. DOI:10.1107/S0021889811038970

40 KOJIMA, Akihiro, Kenjiro TESHIMA, Yasuo SHIRAI a Tsutomu MIYASAKA. Organometal Halide Perovskites as Visible-Light Sensitizers for Photovoltaic Cells. *Journal of the American Chemical Society*. 2009, **131**(17), 6050-6051. ISSN 0002-7863. DOI:10.1021/ja809598r

41 KIM, Hui-Seon, Chang-Ryul LEE, Jeong-Hyeok IM, et al. Lead Iodide Perovskite Sensitized All-Solid-State Submicron Thin Film Mesoscopic Solar Cell with Efficiency Exceeding 9%. *Scientific Reports*. 2012, **2**(1). ISSN 2045-2322. DOI:10.1038/srep00591

42 LIU, Dianyi a Timothy L. KELLY. Perovskite solar cells with a planar heterojunction structure prepared using room-temperature solution processing techniques. *Nature Photonics*. 2014, **8**(2), 133-138. ISSN 1749-4885. DOI:10.1038/nphoton.2013.342

43 LIU, Mingzhen, Michael B. JOHNSTON a Henry J. SNAITH. Efficient planar heterojunction perovskite solar cells by vapour deposition. *Nature*. 2013, **501**(7467), 395-398. ISSN 0028-0836. DOI:10.1038/nature12509

44 SAUVÉ, Geneviève a Roshan FERNANDO. Beyond Fullerenes: Designing Alternative Molecular Electron Acceptors for Solution-Processable Bulk Heterojunction Organic Photovoltaics. *The Journal of Physical Chemistry Letters*. 2015, **6**(18), 3770-3780. ISSN 1948-7185. DOI:10.1021/acs.jpclett.5b01471

45 HOPPE, Harald a N. Serdar SARICIFTCI. Polymer Solar Cells. *Photoresponsive Polymers II*. Berlin, Heidelberg: Springer Berlin Heidelberg, 2008, 2007-10-17, 1-86. ISBN 978-3-540-69452-6. DOI:10.1007/12_2007_121

46 SINGH, Ram Prakash a Omkar Singh KUSHWAHA. Polymer Solar Cells: An Overview. *Macromolecular Symposia*. 2013, **327**(1), 128-149. ISSN 10221360. DOI:10.1002/masy.201350516

47 MIYATA, Atsuhiko, Anatolie MITIOGLU, Paulina PLOCHOCKA, Oliver PORTUGALL, Jacob Tse-Wei WANG, Samuel D. STRANKS, Henry J. SNAITH a Robin J. NICHOLAS. Direct measurement of the exciton binding energy and effective masses for charge carriers in organic–

inorganic tri-halide perovskites. *Nature Physics*. 2015, **11**(7), 582-587. ISSN 1745-2473. DOI:10.1038/nphys3357

48 EDRI, Eran, Saar KIRMAYER, Sabyasachi MUKHOPADHYAY, Konstantin GARTSMAN, Gary HODES a David CAHEN. Elucidating the charge carrier separation and working mechanism of CH3NH3PbI3−xClx perovskite solar cells. *Nature Communications*. 2014, **5**(1). ISSN 2041-1723. DOI:10.1038/ncomms4461

49 LIN, Qianqian, Ardalan ARMIN, Ravi Chandra Raju NAGIRI, Paul L. BURN a Paul MEREDITH. Electro-optics of perovskite solar cells. *Nature Photonics*. 2015, **9**(2), 106-112. ISSN 1749-4885. DOI:10.1038/nphoton.2014.284

50 JUAREZ-PEREZ, Emilio J., Rafael S. SANCHEZ, Laura BADIA, Germá GARCIA-BELMONTE, Yong Soo KANG, Ivan MORA-SERO a Juan BISQUERT. Photoinduced Giant Dielectric Constant in Lead Halide Perovskite Solar Cells. *The Journal of Physical Chemistry Letters*. 2014, **5**(13), 2390-2394. ISSN 1948-7185. DOI:10.1021/jz5011169

51 MARINOVA, Nevena, Silvia VALERO a Juan Luis DELGADO. Organic and perovskite solar cells: Working principles, materials and interfaces. *Journal of Colloid and Interface Science*. 2017, **488**, 373-389. ISSN 00219797. DOI:10.1016/j.jcis.2016.11.021

52 HOU, Jianhui, Olle INGANÄS, Richard H. FRIEND a Feng GAO. Organic solar cells based on non-fullerene acceptors. *Nature Materials*. 2018, **17**(2), 119-128. ISSN 1476-1122. DOI:10.1038/nmat5063

53 YAN, Cenqi, Stephen BARLOW, Zhaohui WANG, He YAN, Alex K.-Y. JEN, Seth R. MARDER a Xiaowei ZHAN. Non-fullerene acceptors for organic solar cells. *Nature Reviews Materials*. 2018, **3**(3). ISSN 2058-8437. DOI:10.1038/natrevmats.2018.3

54 YE, Long, Huizhen KE a Yang LIU. The renaissance of polythiophene organic solar cells. *Trends in Chemistry*. 2021, **3**(12), 1074-1087. ISSN 25895974. DOI:10.1016/j.trechm.2021.09.008

55 NIU, Guangda, Wenzhe LI, Fanqi MENG, Liduo WANG, Haopeng DONG a Yong QIU. Study on the stability of CH 3 NH 3 PbI 3 films and the effect of post-modification by aluminum oxide in all-solid-state hybrid solar cells. *J. Mater. Chem. A*. 2014, **2**(3), 705-710. ISSN 2050-7488. DOI:10.1039/C3TA13606J

56 SCHULZ, Philip, David CAHEN a Antoine KAHN. Halide Perovskites: Is It All about the Interfaces?. *Chemical Reviews*. 2019, **119**(5), 3349-3417. ISSN 0009-2665. DOI:10.1021/acs.chemrev.8b00558

57 WANG, Rui, Jianhui QIAO, Bizu HE, Xiaosheng TANG, Fei WU a Linna ZHU. Electron extraction layer based on diketopyrrolopyrrole/isoindigo to improve the efficiency of inverted perovskite solar cells. *Journal of Materials Chemistry C*. 2018, **6**(31), 8429-8434. ISSN 2050-7526. DOI:10.1039/C8TC02766H

58 SMITH, Timothy J. a Keith J. STEVENSON. Reference Electrodes. *Handbook of Electrochemistry*. Elsevier, 2007, 2007, s. 73-110. ISBN 9780444519580. DOI:10.1016/B978-044451958-0.50005-7

59 CARDONA, Claudia M., Wei LI, Angel E. KAIFER, David STOCKDALE a Guillermo C. BAZAN. Electrochemical Considerations for Determining Absolute Frontier Orbital Energy Levels of Conjugated Polymers for Solar Cell Applications. *Advanced Materials*. 2011, **23**(20), 2367-2371. ISSN 09359648. DOI:10.1002/adma.201004554

60 HAN, Xiao, Qing BAI, Liang YAO, et al. Highly Efficient Solid-State Near-Infrared Emitting Material Based on Triphenylamine and Diphenylfumaronitrile with an EQE of 2.58% in Nondoped Organic Light-Emitting Diode. *Advanced Functional Materials*. 2015, **25**(48), 7521-7529. ISSN 1616301X. DOI:10.1002/adfm.201503344

61 ZHANG, Yilin, Meijuan JIANG, Guang-Chao HAN, Ke ZHAO, Ben Zhong TANG a Kam Sing WONG. Solvent Effect and Two-Photon Optical Properties of Triphenylamine-Based Donor–Acceptor Fluorophores. *The Journal of Physical Chemistry C*. 2015, **119**(49), 27630-27638. ISSN 1932-7447. DOI:10.1021/acs.jpcc.5b06762

62 KONG, Lin, JiaXiang YANG, HongPing ZHOU, et al. Synthesis, photophysical properties and TD-DFT calculation of four two-photon absorbing triphenylamine derivatives. *Science China Chemistry*. 2013, **56**(1), 106-116. ISSN 1674-7291. DOI:10.1007/s11426-012-4794-4

63 LU, Liangde, Rene J. LACHICOTTE, Thomas L. PENNER, Jerry PERLSTEIN a David G. WHITTEN. Exciton and Charge-Transfer Interactions in Nonconjugated Merocyanine Dye Dimers: Novel Solvatochromic Behavior for Tethered Bichromophores and Excimers. *Journal of the American Chemical Society*. 1999, **121**(36), 8146-8156. ISSN 0002-7863. DOI:10.1021/ja983778h

64 GIERSCHNER, Johannes a Soo Young PARK. Luminescent distyrylbenzenes: tailoring molecular structure and crystalline morphology. *Journal of Materials Chemistry C*. 2013, **1**(37), 5818–5832. ISSN 2050-7526. DOI:10.1039/c3tc31062k

65 CHENG, Xiao, Di LI, Zhenyu ZHANG, Hongyu ZHANG a Yue WANG. Organoboron Compounds with Morphology-Dependent NIR Emissions and Dual-Channel Fluorescent ON/OFF Switching. *Organic Letters*. 2014, **16**(3), 880-883. ISSN 1523-7060. DOI:10.1021/ol403639n

66 PAUK, Karel, Stanislav LUŇÁK, Aleš RŮŽIČKA, et al. Green-, Red-, and Infrared-Emitting Polymorphs of Sterically Hindered Push–Pull Substituted Stilbenes. *Chemistry – A European Journal*. 2021, **27**(13), 4341-4348. ISSN 0947-6539. DOI:10.1002/chem.202004419

67 LIU, Pei, Peng ZHANG, Dongliang CAO, Lihua GAN a Yuanfang LI. New side groups-tuned triphenylamine-based chromophores: Synthesis, morphology, photophysical properties and electronic structures. *Journal of Molecular Structure*. 2013, **1050**, 151-158. ISSN 00222860. DOI:10.1016/j.molstruc.2013.07.031

68 CHIANG, C.-L., M.-F. WU, D.-C. DAI, Y.-S. WEN, J.-K. WANG a C.-T. CHEN. Red-Emitting Fluorenes as Efficient Emitting Hosts for Non-Doped, Organic Red-Light-Emitting Diodes. *Advanced Functional Materials*. 2005, **15**(2), 231-238. ISSN 1616-301X. DOI:10.1002/adfm.200400102

69 HESTAND, Nicholas J. a Frank C. SPANO. Expanded Theory of H- and J-Molecular Aggregates: The Effects of Vibronic Coupling and Intermolecular Charge Transfer. *Chemical Reviews*. 2018, **118**(15), 7069-7163. ISSN 0009-2665. DOI:10.1021/acs.chemrev.7b00581

70 LUŇÁK JR., Stanislav, Lukáš HAVEL, Jan VYŇUCHAL, Petra HORÁKOVÁ, Jiří KUČERÍK, Martin WEITER a Radim HRDINA. The geometry and absorption of diketo-pyrrolo-pyrroles substituted with various aryls. *Dyes and Pigments*. 2010, **85**(1-2), 27-36. ISSN 01437208. DOI:10.1016/j.dyepig.2009.09.014

71 KRATOCHVIL, Matous, Martin CIGANEK, Cigdem YUMUSAK, et al. Near-infrared absorbing hydrogen-bonded dithioketopyrrolopyrrole (DTPP) n-type semiconductors. *Dyes and Pigments*. 2022, **197**, 109884. ISSN 01437208. DOI:10.1016/j.dyepig.2021.109884

72 HOOVER, Gabrielle C. a Dwight S. SEFEROS. Photoactivity and optical applications of organic materials containing selenium and tellurium. *Chemical Science*. 2019, **10**(40), 9182-9188. ISSN 2041-6520. DOI:10.1039/C9SC04279B

73 JEON, Nam Joong, Jun Hong NOH, Young Chan KIM, Woon Seok YANG, Seungchan RYU a Sang Il SEOK. Solvent engineering for high-performance inorganic–organic hybrid perovskite solar cells. *Nature Materials*. 2014, **13**(9), 897-903. ISSN 1476-1122. DOI:10.1038/nmat4014

74 WALDAUF, C., P. SCHILINSKY, M. PERISUTTI, J. HAUCH a C.J. BRABEC. Solution-Processed Organic n-Type Thin-Film Transistors. *Advanced Materials*. 2003, **15**(24), 2084-2088. ISSN 0935-9648. DOI:10.1002/adma.200305623

75 RAUH, Daniel, Alexander WAGENPFAHL, Carsten DEIBEL a Vladimir DYAKONOV. Relation of open circuit voltage to charge carrier density in organic bulk heterojunction solar cells. *Applied Physics Letters*. 2011, **98**(13), 133301. ISSN 0003-6951. DOI:10.1063/1.3566979

8 CURRICULUM VITAE

Education

2017–present: Doctoral studies at the Faculty of Chemistry of the Brno University of Technology, majoring in Chemistry, Technology and Properties of Materials

2015–2017: Master degree at the FCH, BUT, majoring in Consumer Chemistry

2012–2015: Bachelor degree at the FCH, BUT, majoring in Consumer Chemistry

Work experience

2017–present: Employment as researcher at FCH,

International experience

2019: Research internship at LIOS, Linz, research topic – use of organic semiconductors in perovskite photonics

2016: ERASMUS+ study stay at the Instituto Superior Técnico in Lisbon.

Awards

Josef Hlávka Award for the diploma thesis.
Scholarship within the Brno Ph.D. Talent program awarded by the Statutory City of Brno.